

The Yeast Snt2 Protein Coordinates the Transcriptional Response to Hydrogen Peroxide-Mediated Oxidative Stress

Lindsey A. Baker, Beatrix M. Ueberheide, Scott Dewell, Brian T. Chait, Deyou Zheng and C. David Allis
Mol. Cell. Biol. 2013, 33(19):3735. DOI: 10.1128/MCB.00025-13.
Published Ahead of Print 22 July 2013.

Updated information and services can be found at:
<http://mcb.asm.org/content/33/19/3735>

SUPPLEMENTAL MATERIAL	<i>These include:</i> Supplemental material
REFERENCES	This article cites 65 articles, 25 of which can be accessed free at: http://mcb.asm.org/content/33/19/3735#ref-list-1
CONTENT ALERTS	Receive: RSS Feeds, eTOCs, free email alerts (when new articles cite this article), more»

Information about commercial reprint orders: <http://journals.asm.org/site/misc/reprints.xhtml>
To subscribe to to another ASM Journal go to: <http://journals.asm.org/site/subscriptions/>

The Yeast Snt2 Protein Coordinates the Transcriptional Response to Hydrogen Peroxide-Mediated Oxidative Stress

Lindsey A. Baker,^a Beatrix M. Ueberheide,^{b*} Scott Dewell,^c Brian T. Chait,^b Deyou Zheng,^d C. David Allis^a

Laboratory of Chromatin Biology & Epigenetics, The Rockefeller University, New York, New York, USA^a; Laboratory of Mass Spectrometry and Gaseous Ion Chemistry, The Rockefeller University, New York, New York, USA^b; Genomics Resource Center, The Rockefeller University, New York, New York, USA^c; Departments of Neurology, Genetics, and Neuroscience, Albert Einstein College of Medicine, Bronx, New York, USA^d

Regulation of gene expression is a vital part of the cellular stress response, yet the full set of proteins that orchestrate this regulation remains unknown. Snt2 is a *Saccharomyces cerevisiae* protein whose function has not been well characterized that was recently shown to associate with Ecm5 and the Rpd3 deacetylase. Here, we confirm that Snt2, Ecm5, and Rpd3 physically associate. We then demonstrate that cells lacking Rpd3 or Snt2 are resistant to hydrogen peroxide (H₂O₂)-mediated oxidative stress and use chromatin immunoprecipitation followed by high-throughput sequencing (ChIP-seq) to show that Snt2 and Ecm5 recruit Rpd3 to a small number of promoters and in response to H₂O₂, colocalize independently of Rpd3 to the promoters of stress response genes. By integrating ChIP-seq and expression analyses, we identify target genes that require Snt2 for proper expression after H₂O₂. Finally, we show that cells lacking Snt2 are also resistant to nutrient stress imparted by the TOR (target of rapamycin) pathway inhibitor rapamycin and identify a common set of genes targeted by Snt2 and Ecm5 in response to both H₂O₂ and rapamycin. Our results establish a function for Snt2 in regulating transcription in response to oxidative stress and suggest Snt2 may also function in multiple stress pathways.

The ability of cells to respond to stressful conditions is crucial to survival and involves both the rapid activation of stress defense proteins to begin detoxifying or protecting against the stress and gene expression changes, which bolster the stress response but take longer to manifest. In the budding yeast, *Saccharomyces cerevisiae*, numerous types of stress, including heat shock, oxidative stress, and nitrogen starvation, promote similar changes in a core set of genes called the “environmental stress response” (ESR) genes (1, 2). As part of the ESR, genes involved in RNA processing, translation, and ribosomal biogenesis are repressed, while genes involved in carbohydrate metabolism, protein folding, detoxification of reactive oxygen species (ROS), and maintaining redox balance are activated. These changes redirect energy away from basic metabolism toward stress detoxification and adaptation.

While the ESR is enacted similarly in response to diverse stresses, the levels and timing of gene expression changes vary depending on the type of stress, and distinct stresses promote additional changes in unique sets of genes (1). For example, while genes involved in ROS detoxification are all activated as part of the ESR, these genes are activated at higher levels when cells are exposed to oxidative stress through treatment with H₂O₂ (1). The stress-specific differences in the timing and extent of gene expression changes suggest that complex mechanisms regulate the ESR.

While numerous chromatin and transcriptional regulators have been linked to stress gene regulation (3–5), the full complement of proteins involved in this crucial function remains unknown. The yeast Snt2 protein was previously found to be enriched at promoter regions (6), suggesting that Snt2 may regulate transcription. In addition, Snt2 was recently reported to interact with Ecm5 and the Rpd3 deacetylase (7). Ecm5 was identified in a screen for cell wall mutants (8), but like Snt2, it contains protein domains expected to associate with chromatin (Fig. 1A). Rpd3 is a lysine deacetylase known to associate with two other well-characterized complexes, Rpd3 large [Rpd3(L)] and Rpd3 small [Rpd3(S)] (9–11). The Rpd3(L) complex has been reported to

function in numerous pathways and notably has been linked to ESR regulation (12–16). However, the function of Snt2, either on its own or in association with Ecm5 and Rpd3, remains unclear.

Multiple lines of evidence point to a role for Snt2 in the oxidative stress response or possibly in the ESR more generally. First, deletion of Snt2’s reported interaction partner *ECM5* results in synthetic sickness when combined with deletion of *ASK10* (17), a gene originally identified as a high-copy-number enhancer of the Skn7 stress transcription factor that is involved in the oxidative stress response (18, 19). In addition, *snt2Δ* cells have increased phosphorylation of Slt2 (20), a mitogen-activated protein kinase (MAPK) phosphorylated in response to oxidative and other stresses (21). Finally, an integrated pathway analysis based on published stress-induced transcription changes and Snt2 genomic localization data reported a link between Snt2 and the osmotic stress response (22).

We set out to determine whether Snt2 was involved in regulating the transcriptional response to oxidative stress. We first confirmed that Snt2 physically associated with Ecm5 and Rpd3 and found that cells lacking Snt2 or Rpd3 were resistant to H₂O₂-mediated oxidative stress. To better understand how Snt2 and Ecm5 might function during stress, we used chromatin immuno-

Received 7 January 2013 Returned for modification 3 February 2013

Accepted 16 July 2013

Published ahead of print 22 July 2013

Address correspondence to C. David Allis, alliscd@mail.rockefeller.edu.

* Present address: Beatrix M. Ueberheide, Department of Biochemistry and Molecular Pharmacology, NYU School of Medicine, New York, New York, USA.

Supplemental material for this article may be found at <http://dx.doi.org/10.1128/MCB.00025-13>.

Copyright © 2013, American Society for Microbiology. All Rights Reserved.

doi:10.1128/MCB.00025-13

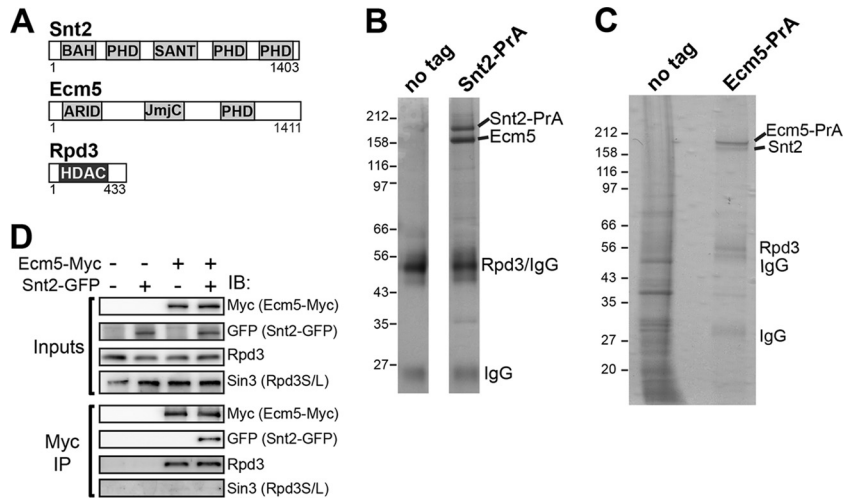


FIG 1 Snt2 associates with Ecm5 and the Rpd3 deacetylase. (A) Domain structures of Snt2, Ecm5, and Rpd3. BAH, bromo-adjacent homology; PHD, plant homeodomain finger; SANT, Spt3–Ada3–N-CoR–TFIIS (N-CoR stands for nuclear receptor corepressor 1, and TFIIS stands for transcription elongation factor IIS); ARID, AT-rich interaction domain; JmjC, Jumonji C; HDAC, histone deacetylase. (B) Silver-stained SDS-polyacrylamide gels of eluents from Snt2-PrA and control (no tag) affinity purifications. Proteins identified by LC-MS are listed next to bands of the appropriate size. Rpd3 comigrated on the gel with IgG. Numbers to the left are molecular mass in kilodaltons. (C) Coomassie blue-stained gel analysis of Ecm5-PrA and control purifications. Proteins identified by LC-MS are listed next to the corresponding bands. (D) Lysates of untagged, Ecm5-Myc, Snt2-GFP, or Ecm5-Myc Snt2-GFP strains were immunoprecipitated with anti-Myc antibody, and inputs and immunoprecipitates (IPs) were immunoblotted (IB) with anti-Myc (to detect Ecm5), anti-GFP (to detect Snt2), anti-Rpd3, or anti-Sin3.

precipitation followed by high-throughput sequencing (ChIP-seq) to map the genomic localizations of each protein before and 30 min after H_2O_2 treatment, and we identified two categories of promoters targeted by Snt2 and Ecm5, promoters very highly enriched for Snt2 and Ecm5 regardless of stress, at which both proteins were required to recruit Rpd3, and promoters at which Snt2 and Ecm5 localized independently of Rpd3 in response to H_2O_2 stress. RNA-sequencing (RNA-seq) analysis identified target genes that required Snt2 for proper expression changes in H_2O_2 stress, including genes involved in the ESR. Finally, the *snt2Δ* strain was also resistant to nutrient stress imparted by the TOR (target of rapamycin) pathway inhibitor rapamycin, and rapamycin treatment enhanced Snt2 and Ecm5 localization to a subset of the H_2O_2 target promoters. Our results identify a role for Snt2 in regulating transcription in response to oxidative stress and further suggest that Snt2 may have broad roles in stress gene regulation.

MATERIALS AND METHODS

Strains, growth conditions, and growth assays. All *S. cerevisiae* strains used in this work (Table 1) were derived from the S288C background strain and are isogenic with BY4741. Where noted, deletion strains were obtained from Open Biosystems. Otherwise, strains were generated by using standard genetic methods (23). Deletion strains were constructed by replacing the gene of interest with a PCR-amplified *KanMX4* or *HygMX4* marker through homologous recombination. Tagged strains were created by targeting PCR-amplified protein A (PrA), green fluorescent protein (GFP), or 13Myc (13 copies of the Myc epitope) tags to the 3' ends of genes of interest, as previously described (23, 24). All strains were confirmed by PCR. Except where otherwise indicated, cells were grown in standard YPD medium (1% yeast extract, 2% peptone, and 2% glucose). For rapamycin experiments, cultures were grown in synthetic defined medium supplemented with complete supplement mixture (synthetic defined medium plus amino acid supplement mixture CSM [SD CSM]; CSM from MP Biomedicals).

For plate spotting assays, saturated overnight cultures of each strain

were diluted in YPD (for H_2O_2 plate assays) or SD CSM (for rapamycin plate assays) and grown for 5 to 6 h to mid-log phase (optical density at 600 nm [OD_{600}] = 0.6). The strains were then diluted to 5×10^6 cells/ml and used to make 5-fold serial dilutions. Four microliters of each dilution was spotted onto plates supplemented as indicated in the figure legends. The plates were poured no more than 20 h prior to spotting. H_2O_2 and

TABLE 1 Yeast strains used in this study^a

Strain	Relevant genotype	Source or reference
BY4741	<i>MATa his3Δ1 leu2Δ0 met15Δ0 ura3Δ0</i>	Open Biosystems
LBY101	<i>MATa ECM5-PrA::HIS5</i>	This study
LBY102	<i>MATa SNT2-PrA::HIS5</i>	This study
LBY103	<i>MATa RPD3-PrA::HIS5</i>	This study
LBY104	<i>MATa ECM5-13MYC::KAN</i>	This study
LBY105	<i>MATa SNT2-13MYC::KAN</i>	This study
LBY106	<i>MATa SNT2-GFP::NAT</i>	This study
LBY107	<i>MATa ECM5-13MYC::KAN SNT2-GFP::NAT</i>	This study
LBY108	<i>MATa ecm5Δ::KAN</i>	Open Biosystems
LBY109	<i>MATa snt2Δ::KAN</i>	Open Biosystems
LBY110	<i>MATa rpd3Δ::KAN</i>	This study
LBY111	<i>MATa yap1Δ::KAN</i>	Open Biosystems
LBY112	<i>MATa gpr1Δ::KAN</i>	Open Biosystems
LBY113	<i>MATa sin3Δ::KAN</i>	Open Biosystems
LBY114	<i>MATa sap30Δ::KAN</i>	Open Biosystems
LBY115	<i>MATa cti6Δ::KAN</i>	Open Biosystems
LBY116	<i>MATa snt2Δ::KAN ecm5Δ::HYG</i>	This study
LBY117	<i>MATa snt2Δ::KAN rpd3Δ::HYG</i>	This study
LBY118	<i>MATa rpd3Δ::KAN ecm5Δ::HYG</i>	This study
LBY119	<i>MATa RPD3-13MYC::KAN</i>	This study
LBY120	<i>MATa RPD3-13MYC::KAN snt2Δ::HYG</i>	This study
LBY121	<i>MATa RPD3-13MYC::KAN ecm5Δ::HYG</i>	This study
LBY122	<i>MATa SDS3-13MYC::KAN</i>	This study
LBY123	<i>MATa SDS3-13MYC::KAN snt2Δ::HYG</i>	This study

^a All strains isogenic to strain BY4741.

rapamycin plate assays were imaged after 2 and 3 days, respectively. Survival assays were performed as previously described (25), except that survival was determined after treatment with 0.4 mM H₂O₂ for 4 h.

Affinity purification of Snt2, Ecm5, and Rpd3. *S. cerevisiae* BY4741 and cultures of strains in which Snt2 was tagged with PrA at its C terminus (Snt2-PrA), Ecm5 was tagged with PrA at its C terminus (Ecm5-PrA), or Rpd3 was tagged with PrA at its C terminus (Rpd3-PrA) were prepared for lysis and lysed under cryogenic conditions using a Retsch PM 100 planetary ball mill as described previously (26). Twenty grams of each lysate was resuspended in 100 ml lysis buffer (20 mM HEPES [pH 7.4], 2 mM MgCl₂, 300 mM NaCl, 0.1% Triton X-100, 0.1% Tween 20, 110 mM potassium acetate, 0.1 mg/ml phenylmethylsulfonyl fluoride [PMSF], 2 µg/ml pepstatin, 0.5% protease inhibitor cocktail for fungal and yeast cells [Sigma]), homogenized for 10 s with a Polytron homogenizer, incubated for 10 min with 600 units of recombinant DNase I (Roche), and clarified by centrifugation. Clarified lysates were mixed with equilibrated Dynabeads (Invitrogen) that had been conjugated with rabbit IgG as described previously (27). The rest of the purification was performed as described previously (28).

Mass spectrometric analysis of affinity purifications. For Snt2-PrA, Rpd3-PrA, and control purifications, the eluents were concentrated to dryness using a Speedvac. The eluents were resuspended in 100 mM ammonium bicarbonate, reduced with 20 mM dithiothreitol (DTT) for 1 h at 57°C, and alkylated with 45 mM iodoacetamide for 45 min in the dark at room temperature. The samples were digested with sequencing-grade modified trypsin (Promega) for 8 h at 37°C, and digestion was stopped by acidifying the solution with glacial acetic acid. The solution was pressure loaded onto self-packed precolumns (360 by 75 µm), rinsed with 0.5% acetic acid to remove salt and butt connected to a nano-high-performance liquid chromatography (nano-HPLC) column with integrated 15-µm emitter (360 by 75 µm PicoTip emitter; New Objective) packed with 6 cm of 5-µm C18 beads (YMC ODS AQ). The peptides were eluted with a linear gradient of 0 to 40% solvent B in 50 min and 40 to 100% solvent B in 70 min (solvent A is 0.1 M acetic acid, and solvent B is 70% acetonitrile in 0.1 M acetic acid) using an Agilent 1100 binary HPLC and analyzed on a Finnigan LTQ-XL mass spectrometer (Thermo Fisher) equipped with a nano-HPLC microelectrospray ionization source. The mass spectrometer was operated in a data-dependent mode where one full-scan mass spectrum was followed by 10 collision-activated dissociation (CAD) mass spectra of the 10 most abundant ions. The fragmented ions were set on an exclusion list for 40 s, and the cycle repeated throughout the data acquisition. The resulting spectra were searched against the *Saccharomyces cerevisiae* database using the search algorithm X! Tandem (29). Proteins that have been previously reported to be contaminants of PrA affinity purifications (7, 30), that were identified in a control purification from an untagged cell lysate, or that are known to be highly abundant in yeast cells (31) were assumed to be contaminants.

For the Ecm5-PrA purification, eluents were reduced and alkylated as described above, immediately separated by SDS-PAGE, and stained with Coomassie blue. Stained bands were excised, destained with 50% methanol in 100 mM ammonium bicarbonate, dehydrated, and digested overnight at room temperature in 100 mM ammonium bicarbonate with 50 ng sequencing-grade modified trypsin. Digestions were stopped by adding an aqueous solution of 5% formic acid, 0.2% trifluoroacetic acid (vol/vol), and reverse-phase resin (POROS 20 R2; Perceptive Biosystems). After light shaking at 4°C for 4 h, the resin was washed with 0.5% acetic acid, and bound peptides were eluted first with 40% acetonitrile and then with 80% acetonitrile in 0.5% acetic acid. The eluents were combined and concentrated in a Speedvac. The concentrate was pressure loaded onto a nano-HPLC column, and peptides were separated and identified as described above. The resulting spectra were searched using Sequest in the Proteome Discoverer software package (Thermo Fisher). For further validation of the Rpd3-PrA purification, 50% of the final elution was treated as described for the Ecm5-PrA immunoprecipitation (IP), with focus on

excising the bands with the molecular weights of Ecm5 and Snt2, and spectra were searched using the X! Tandem search algorithm.

Immunoprecipitations and immunoblotting. For the immunoprecipitations, strains were grown to mid-log phase and collected by centrifugation. Cells were resuspended in the lysis buffer described for the affinity purifications, and lysates were prepared by glass bead disruption and clarified by centrifugation. A portion of each clarified lysate was reserved for input. For Ecm5-Myc IPs, the remaining lysates were incubated with anti-c-Myc beads (Sigma) for 1 h at 4°C and washed and eluted as described for the affinity purifications. For Rpd3 IPs, lysates were incubated with either anti-Rpd3 antibody (sc6655; Santa Cruz) or with goat IgG (sc2028; Santa Cruz) for 1 h at 4°C, after which protein G Dynabeads (Invitrogen) were added and allowed to incubate for another hour at 4°C. Rpd3 IPs were washed as described for Ecm5-Myc IPs. The following antibodies were used for immunoblotting: anti-MYC 9E10 (catalog no. 05-419; Millipore), anti-GFP B2 (catalog no. sc9996; Santa Cruz), anti-Rpd3 (catalog no. sc6655; Santa Cruz), anti-Sin3 (catalog no. sc17637; Santa Cruz), and anti-beta actin (catalog no. ab8224; Abcam).

Chromatin immunoprecipitation. For the H₂O₂ ChIP-seq, *S. cerevisiae* BY4741 and strains in which Snt2 was tagged with 13 copies of the Myc epitope (Snt2-Myc) or Ecm5 was tagged with 13 copies of the Myc epitope (Ecm5-Myc) were grown to mid-log phase (OD₆₀₀ = 0.4), and an aliquot of each culture was removed and fixed for ChIP. The remaining cultures were treated with H₂O₂ (final concentration of 0.4 mM) for 30 min and then fixed similarly to the untreated samples. All samples were fixed by adding formaldehyde to a final concentration of 1% and incubating at room temperature for 20 min with rotation. Fixation was quenched by adding glycine to a final concentration of 125 mM. Cells were then pelleted, washed 4 times in cold phosphate-buffered saline (PBS), flash frozen, and stored at -80°C.

For the Ecm5/Snt2-Myc rapamycin ChIP-seq, cultures of each strain were grown to mid-log phase in SD CSM medium, and an aliquot was taken and fixed as described above. Each culture was then split into two cultures: one culture was treated with dimethyl sulfoxide (DMSO), while the other was treated with rapamycin dissolved in DMSO (50 nM [final concentration]). After 30 min, these cultures were fixed for ChIP as described above.

ChIP was performed essentially as described previously (32). Briefly, after lysing cells using 0.5-mm zirconia/silica beads (Biospec Products), chromatin was sonicated using a Bioruptor sonicator to 150- to 500-bp fragments. Chromatin was incubated overnight at 4°C with the Myc 9E10 monoclonal antibody (catalog no. 05-419; Millipore) and then for 2 h with protein G Magna ChIP beads (Millipore). After the DNA was washed and eluted, input and ChIP DNA samples were incubated for 15 h at 65°C to reverse cross-links and then purified using Qiagen PCR purification columns per the manufacturer's instructions. Samples were incubated with RNase at 37°C for 2 h and then purified over Qiagen columns a second time.

Sequencing libraries of input and ChIP DNAs were prepared using the Illumina TruSeq DNA kit per the manufacturer's instructions except that 4% of recommended DNA adapter index concentration and 20% of the recommended PCR primer cocktail concentration were used per library. For the final amplification step, 20 and 21 cycles of PCR were used for the H₂O₂ and rapamycin libraries, respectively. Sequencing was performed on an Illumina HiSeq 2000, and data were analyzed following the Illumina pipeline.

Independent ChIP replicates were performed as described above and analyzed by quantitative PCR (qPCR) on an Applied Biosystems StepOnePlus real-time PCR system using Power SYBR green PCR master mix (Applied Biosystems) per the manufacturer's instructions. For Rpd3-Myc ChIP experiments, cells were fixed for 45 min at room temperature in a solution consisting of 10 mM dimethyl adipimidate (DMA) and 0.25% DMSO in PBS, followed by fixation in 1% formaldehyde for 12 h. Relative enrichment was determined by dividing the percent input at the locus of interest by the percent input at the right arm of telomere 6, which had low

but detectable levels of enrichment for Snt2, Ecm5, and Rpd3, and served as a control for IP efficiency. Sequences of primers used for qPCR are available upon request.

RNA sequencing. BY4741, *ecm5Δ*, and *snt2Δ* cultures were treated with H₂O₂ as described for ChIP-seq experiments. RNA was isolated by hot acidic phenol extraction (33). Sequencing libraries were prepared from 4 μg total RNA using an Illumina TruSeq RNA kit per the manufacturer's instructions. For the final amplification step, 15 cycles of PCR were used. An aliquot of each RNA sample was also reverse transcribed into cDNA using the Superscript III first-strand synthesis system (Invitrogen), and RNA-seq expression values were confirmed by qPCR. Expression qPCRs were performed as described above for ChIP-qPCRs, and the levels of expression of genes of interest were normalized to the levels of *ACT1* expression.

Sequencing analysis. ChIP-seq reads were aligned to the *S. cerevisiae* genome using the Bowtie alignment software (34). Only unique reads that mapped to a single location with no more than 2 mismatches were kept. Regions enriched for Snt2 or Ecm5 binding (i.e., peaks) were called using the MACS (model-based analysis of ChIP-Seq) algorithm (35). Overlapping peaks were defined as peaks whose chromosomal coordinates overlapped by at least 200 bp, as determined using the Galaxy Server (36–38). For Snt2/Ecm5 correlation scatterplots, for each peak of either Snt2 or Ecm5 enrichment, we computed the number of Snt2 or Ecm5 reads per 1,000,000 total reads per peak size in kb (RPKM) using BedTools (39), and used the RPKM values to determine Pearson's correlation coefficients. To determine peaks where Snt2/Ecm5 enrichment increased or decreased following H₂O₂ treatment, a list of all peaks of shared Snt2/Ecm5 enrichment before or after treatment was compiled, and RPKM values were calculated as described above. The peaks were then separated into the peaks with Snt2 and Ecm5 RPKM values 1.5-fold higher, 1.5-fold lower, or unchanged following H₂O₂ treatment. Gene ontology (GO) analysis was performed using the FuncAssociate program (40). Yeast transcription start site (TSS) and open reading frame (ORF) locations were obtained by querying the Ensembl database (www.ensembl.org). The promoters were defined as the regions from 500 bp upstream of queried TSSs to the TSSs. The coordinates of peak summits (determined by the MACS algorithm) were used to uniquely assign each peak to a promoter, ORF, or neither. To determine average Snt2/Ecm5 enrichment around yeast TSSs, a custom script was used to divide regions surrounding each TSS into 50-bp windows and count the average number of reads at all genes within those windows per million mapped reads. For motif analysis, 100-bp regions centered around peak summits were analyzed using the MEME suite (41). The YEASTRACT program (42) was used to search for transcription factors known to regulate Snt2/Ecm5 target genes.

RNA-seq data were aligned using the software TopHat (43), and gene expression levels and differences were calculated using the Cufflinks and Cuffdiff programs (44). All sequencing tracks were displayed using the Integrative Genomics Viewer (IGV) (45).

Sequencing data accession number. All ChIP-seq and RNA-seq data were submitted to the Gene Expression Omnibus (GEO) (<http://www.ncbi.nlm.nih.gov/geo/>) database under the accession number GSE43002.

RESULTS

Snt2 physically associates with Ecm5 and the Rpd3 deacetylase.

In order to better understand the function of Snt2, we first sought to confirm a previous report that Snt2 interacted with Ecm5 and Rpd3 (7). We tagged the C terminus of Snt2 with a protein A (PrA) tag (Snt2-PrA) (24) and affinity purified Snt2-PrA and associated proteins from cryogenically prepared yeast lysates (Fig. 1B). Liquid chromatography-mass spectrometry (LC-MS) analysis identified both Ecm5 and Rpd3 in the Snt2-PrA purification and not in a control purification from an untagged strain (Table 2; see Data set S1 in the supplemental material). To further confirm these associations, we repeated our affinity purifications using a strain

TABLE 2 Peptides identified copurifying with Snt2-PrA^a

Protein	Log(e) ^d	% protein coverage	No. of unique peptides	No. of total peptides	Phosphorylation site ^b
Ecm5	−560.0	34	44	69	
Snt2	−340.9	21	30	38	S641
Rpd3	−108.2	26	9	15	
Rps21b ^c	−53.2	56	5	7	
Rpp2b ^c	−46.8	50	4	4	
Rpl19b ^c	−40.7	22	4	4	
Rps6b ^c	−35.3	15	3	3	
Rpp2a ^c	−34.0	32	3	3	
Rpl18b ^c	−27.0	17	3	3	

^a Proteins also identified in control purification or known to be contaminants of PrA purifications (7, 30) were omitted.

^b Phosphorylated peptide confirmed by tandem MS (MS-MS).

^c While not previously reported as contaminants, these proteins are highly abundant (31) and are therefore likely contaminants.

^d Log of E score generated by X!Tandem algorithm (29).

in which Ecm5 was tagged with PrA. Consistent with the Snt2-PrA affinity purification, Snt2 and Rpd3 were both identified copurifying with Ecm5-PrA (Fig. 1C; see Data set S1).

Rpd3 is known to associate with two well-characterized protein complexes, Rpd3(L) and Rpd3(S) (9, 10). With the exception of Rpd3, components of the Rpd3(L) and (S) complexes were not identified in Snt2- or Ecm5-PrA affinity purifications (Table 2; see Data set S1 in the supplemental material), suggesting that Snt2 and Ecm5 associate with Rpd3 independently of Rpd3(L) and Rpd3(S). We next performed an affinity purification with a PrA-tagged Rpd3 strain. LC-MS analysis of this purified strain identified 10 out of 12 and 5 out of 5 of the known Rpd3-interacting proteins from the Rpd3(L) and Rpd3(S) complexes, respectively (see Data set S1). In addition, 3 Snt2 and 3 Ecm5 peptides were also identified (see Data set S1). To overcome potential suppression of signal for Snt2 and Ecm5 peptides by more abundant Rpd3-interacting proteins, a portion of the Rpd3-PrA purification was also resolved on an SDS-polyacrylamide gel, and Coomassie blue-stained gel bands corresponding in size to Snt2 and Ecm5 were excised and analyzed by LC-MS, confirming the presence of Snt2 and Ecm5 peptides in the Rpd3-PrA purification (see Data set S1).

To further confirm these results, we generated a strain in which Ecm5 and Snt2 were tagged with 13 copies of the Myc epitope or with a GFP tag, respectively. Myc-tagged Ecm5 (Ecm5-Myc) was immunoprecipitated using a Myc antibody, and immunoblot analysis confirmed that GFP-tagged Snt2 (Snt2-GFP) and Rpd3 both coprecipitated with Ecm5-Myc (Fig. 1D). In contrast, Sin3, a component of the Rpd3(L) and Rpd3(S) complexes, did not coprecipitate with Ecm5-Myc (Fig. 1D). Taken together, our results confirm that Snt2, Ecm5, and Rpd3 physically associate in a form separable from Rpd3(L) and Rpd3(S).

Cells lacking Snt2 or Rpd3 are resistant to H₂O₂-induced oxidative stress. We next sought to determine the function of Snt2, either alone or in association with Ecm5 and Rpd3. A recent genetic screen found that deletion of *ECM5* resulted in synthetic sickness when combined with deletion of the *ASK10* gene (17), which encodes a protein involved in the oxidative stress response (18). Furthermore, cells lacking Snt2 have higher levels of phosphorylation of the stress MAPK Slt2 (20), and a bioinformatics

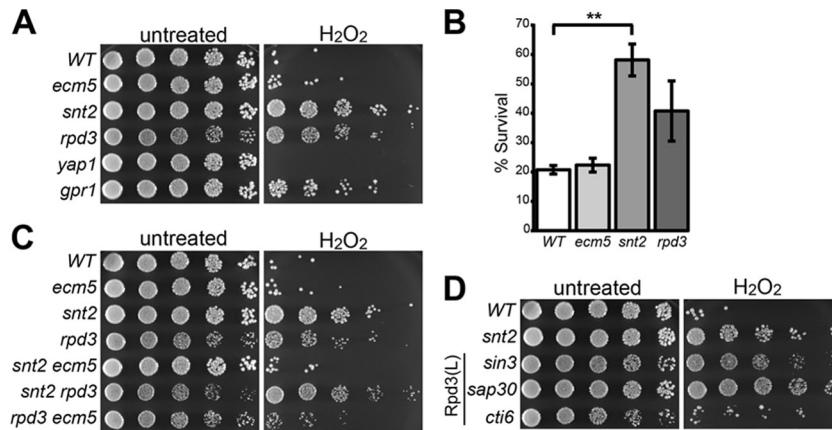


FIG 2 Cells lacking Snt2 or Rpd3 are resistant to H₂O₂. (A) Fivefold serial dilutions of the wild-type (WT) strain or indicated knockout strains were spotted onto YPD plates that were untreated or supplemented with 2.3 mM H₂O₂. Plates were imaged after 2 days. (B) Log-phase cultures of the wild-type strain or indicated knockout strains were treated with 0.4 mM H₂O₂ for 4 h. Percent survival was determined by CFU assay. Data are means \pm standard errors of the means (SEMs) (error bars) from 3 biological replicates. Values that are statistically significantly different ($P < 0.01$) are indicated by the bar and two asterisks. (C and D) Plate spotting assays with the indicated knockout strains were performed as described above for panel A.

study suggested that Snt2 might function to activate genes in response to stress (22). Rpd3 is known to regulate the response to numerous stresses, including oxidative stress, often as a part of the Rpd3(L) complex (12–15). On the basis of these data, we hypothesized that Snt2, Ecm5, and Rpd3 might function as an additional regulator of the oxidative stress response.

To test this hypothesis, we spotted serial dilutions of wild-type, *snt2* Δ , *ecm5* Δ , and *rpd3* Δ strains on untreated or H₂O₂-treated plates. While all the strains grew similarly on untreated plates (with the *rpd3* Δ strain having a slight growth defect), there was marked contrast in the growth of these strains on plates containing H₂O₂ (Fig. 2A). The wild-type and *ecm5* Δ strains showed strong H₂O₂ sensitivity. Consistent with the known role for Rpd3 in regulating the yeast oxidative stress response as part of the Rpd3(L) complex, the *rpd3* Δ strain was resistant to H₂O₂. Strikingly, the *snt2* Δ strain was even more resistant to H₂O₂ than the *rpd3* Δ strain, showing similar levels of resistance to a strain lacking Gpr1, a glucose sensor whose deletion was reported to result in H₂O₂ resistance (46). Consistent with previous reports (47), a strain lacking the oxidative stress transcription factor Yap1 was sensitive to H₂O₂ (Fig. 2A). Separately derived *snt2* Δ and *rpd3* Δ strains constructed on the BY4742 background also showed H₂O₂ resistance in this assay (data not shown).

We next determined whether *snt2* Δ and *rpd3* Δ strains also showed H₂O₂ resistance using a liquid survival CFU assay (25). When wild-type or *ecm5* Δ cells were treated with H₂O₂ at a final concentration of 0.4 mM for 4 h, approximately 20% of cells survived (Fig. 2B). In contrast, the *rpd3* Δ strain had enhanced survival, with an average survival rate of 40.7%. Moreover, greater than 50% of *snt2* Δ cells survived H₂O₂ treatment, a statistically significant difference from the wild-type levels, confirming that cells lacking Snt2 are resistant to oxidative stress.

The differing H₂O₂ sensitivities of the *snt2* Δ , *rpd3* Δ , and *ecm5* Δ mutants suggested that despite their physical association, these proteins might have distinct functions in the oxidative stress pathway. In order to better understand how these proteins function to regulate stress tolerance, we next determined the H₂O₂ resistance of double deletion strains for these factors. Surprisingly, deletion of *ECM5* reversed the H₂O₂ resistance seen in the *snt2* Δ

strain (Fig. 2C), suggesting that Ecm5 has a function in the oxidative stress response that is opposed to the function of Snt2. Although the *snt2* Δ *rpd3* Δ double knockout possessed a modest growth defect similar to that of the *rpd3* Δ strain (as can be seen by the smaller size of the *snt2* Δ *rpd3* Δ colonies in Fig. 2C), the double knockout was more H₂O₂ resistant than the *rpd3* Δ strain alone, showing similar levels of resistance to the *snt2* Δ strain. This result suggests that deletions of *RPD3* and *SNT2* promote stress resistance through different pathways, with the stress resistance of the *rpd3* Δ strain possibly relating to the known role of the Rpd3(L) complex in regulating the oxidative stress response. In agreement, strains lacking the Rpd3(L) complex members Sin3, Sap30, and Cti6 were also H₂O₂ resistant (Fig. 2D). Taken together, these results suggest that even though Snt2, Ecm5, and Rpd3 physically associate in cells, Snt2 performs a function in the oxidative stress response distinct from that of Ecm5 or Rpd3.

Similar levels of Snt2, Ecm5, and Rpd3 associate with one another before and after H₂O₂ treatment. We next determined whether oxidative stress affected the associations between Snt2, Ecm5, and Rpd3. Immunoblot analysis of Ecm5-Myc, Snt2-GFP, and Rpd3 protein levels in Myc immunoprecipitations from *ECM5-MYC SNT2-GFP* or *SNT2-GFP* strains did not reveal significant differences in the levels of Snt2-GFP and Rpd3 associating with Ecm5-Myc before and after H₂O₂ treatment (Fig. 3A). Similarly, when Rpd3 was immunoprecipitated from *ECM5-MYC SNT2-GFP* lysates, there were not differences in the levels of Snt2-GFP and Ecm5-Myc coprecipitating with Rpd3 before and after H₂O₂ stress (Fig. 3B [note that while there was slightly more Ecm5-Myc and Snt2-GFP detected in the immunoprecipitation from the H₂O₂-treated cells, there was also more Rpd3 precipitated]). Thus, H₂O₂ stress does not result in changes in the levels of Snt2, Ecm5, and Rpd3 physically associating with each other.

In response to H₂O₂ stress, Snt2 and Ecm5 colocalize to gene promoters. To better understand how Snt2 and Ecm5 function in the oxidative stress response, we used ChIP-seq to map the genomic localizations of Myc-tagged Snt2 or Ecm5 both before and 30 min after H₂O₂ treatment. We chose to focus on Snt2 and Ecm5 to avoid having to distinguish Rpd3 localization associated with Snt2 and Ecm5 from Rpd3 localization via the Rpd3(L) and

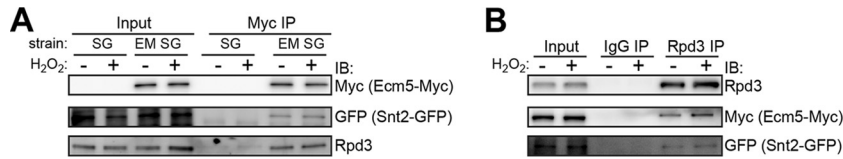


FIG 3 H₂O₂ treatment does not affect the levels of Snt2 and Rpd3 associating with Ecm5 or the levels of Ecm5 and Snt2 associating with Rpd3. (A) Immunoblot analysis of Myc immunoprecipitations from *ECM5-MYC SNT2-GFP* (EM SG) or *SNT2-GFP* (SG) strains that were untreated (–) or treated with H₂O₂ (+). For Ecm5-Myc and Snt2-GFP immunoblots, input is 15% of IP; for Rpd3 immunoblot, input is 1% of IP. (B) Immunoblot analysis of Rpd3 immunoprecipitation from the *ECM5-MYC SNT2-GFP* strain treated as described above for panel A. Inputs are 15% of IPs.

Rpd3(S) complexes. Consistent with their physical association, the Snt2 and Ecm5 ChIP profiles were strikingly similar (representative region shown in Fig. 4A). Both before and after H₂O₂ treatment, the majority of peaks of Snt2 enrichment overlapped with Ecm5 peaks by at least 200 bp (Fig. 4B). Scatterplots confirmed correlations between Snt2 and Ecm5 enrichment levels (Fig. 4C, Pearson's correlations of 0.895 and 0.917 for the 0-min and 30-min data sets, respectively).

We next analyzed the genomic distributions of Snt2 and Ecm5 peaks for enrichment at particular genetic features (Fig. 4D). Before treatment, 43% of peaks fell in promoter regions, while 23% fell within open reading frame (ORF) regions. Reads from an untagged control strain were also enriched in ORF peak regions (data not shown), suggesting that the ORF peaks may be an artifact reflecting the higher accessibility of transcribed chromatin rather than real sites of Snt2/Ecm5 enrichment, an effect that has been previously reported for ChIP experiments involving other proteins (48). We therefore chose to focus on peaks localized to promoter regions for further study. Strikingly, 30 min after H₂O₂ treatment, Snt2 and Ecm5 underwent dramatic localization changes, with many regions showing new or enhanced localization of Snt2 and Ecm5 (Fig. 4A). After H₂O₂ treatment, 74% of peaks were in promoters (Fig. 4D). Alignments of Snt2 and Ecm5 ChIP-seq reads around the transcription start sites (TSSs) of all genes revealed Snt2 and Ecm5 enrichment approximately 250 bp upstream of the TSS in H₂O₂-treated cells (Fig. 4E, dark purple lines). In addition, there were 817 peaks of Snt2 and Ecm5 enrichment identified after treatment, compared to only 315 peaks present before (Fig. 4B). For both Snt2 and Ecm5, the majority of peaks called in untreated samples were also present after H₂O₂ treatment (Fig. 4F).

In order to compare between different ChIP-seq data sets, we generated a list of all peaks of both Snt2 and Ecm5, identified before or after stress, and calculated Snt2 or Ecm5 enrichment at each region before and after stress (see Materials and Methods). When all peaks were considered together, enrichment of Snt2 and Ecm5 was significantly higher after treatment compared to before treatment, consistent with the many new peaks identified in treated cells (Fig. 4G). Similarly, scatterplots showing Snt2 or Ecm5 enrichment at all peak regions before treatment compared to enrichment after treatment show that the majority of peaks had enrichment scores at least 1.5-fold higher after H₂O₂ treatment compared to enrichment before treatment (Fig. 4H [note that purple points outnumber gray and orange points]).

To look for motifs in Snt2/Ecm5 target sites, we used the *de novo* motif finder Meme (41). The 100 bp centered around each peak's summit (determined by the MACS algorithm) was used for this analysis. While no motif was significantly enriched when all peaks were analyzed together, when we used the 20 peaks with the

highest Snt2/Ecm5 enrichment levels for this analysis, a motif containing (A/G)(C/T)GGCGCTA(C/T/A)CA was strongly enriched (Fig. 4I, E value of 1.3×10^{-7}), in agreement with an Snt2-binding motif identified in a previous Snt2 chromatin immunoprecipitation with microarray technology (ChIP-chip) study, (C/T)GGCGCTA(C/T)CA (6). We next analyzed the peaks where Snt2 and Ecm5 levels were at least 1.5-fold higher after H₂O₂ treatment (purple points in Fig. 4H). A second motif, CCG(C/T)GGA, was identified among these H₂O₂-enriched Snt2/Ecm5 peaks (Fig. 4I, right, E value of 1×10^{-3}). This motif is similar to the previously published motifs of the Pdr1 and Pdr3 transcription factors (CCGCGGA) (49), which regulate cellular transport genes (50). Collectively, these results show that H₂O₂ treatment stimulates Snt2 and Ecm5 to colocalize to promoters and identify Pdr1 and Prd3 as potential factors that may cooperate with Snt2 and Ecm5.

After H₂O₂ treatment, Snt2 and Ecm5 localize to promoters of genes involved in oxidative stress and cellular metabolism. We next sought to determine which categories of genes were targeted by Snt2 and Ecm5 as a result of oxidative stress. As described above, we identified peaks in which Snt2/Ecm5 enrichment increased, decreased, or did not change after H₂O₂ treatment (purple, orange, or gray points, respectively, in Fig. 4H), and analyzed each set of target genes using gene ontology (GO) analysis (40). Genes whose promoters had decreased levels of Snt2 and Ecm5 after H₂O₂ stress were involved in protein metabolism (ribosome and translation) (Fig. 4J). Genes whose promoters had similar levels of Snt2 and Ecm5 before and after treatment also functioned in protein metabolism, as well as in carbohydrate metabolism (gluconeogenesis, glycolysis, and transposition [Fig. 4J]). Thus, in unstressed cells, Snt2 and Ecm5 target sugar and protein metabolism genes.

Genes where Snt2 and Ecm5 levels increased after H₂O₂ treatment had functions in amino acid, steroid, and alcohol metabolism (Fig. 4J). For example, after H₂O₂ treatment, Snt2 and Ecm5 were enriched at the promoters of the *BAT2* amino acid metabolism gene and the sterol metabolism genes *ERG3* and *ERG6*, which help synthesize the cell wall component ergosterol (Fig. 5A). While the cell wall category was not identified by GO analysis, we found additional cell wall genes targeted by Snt2 and Ecm5 in response to H₂O₂ treatment, including the cell wall glucanase *SCW10* and the glucan synthase *FKS3* (Fig. 5A). Ecm5 was originally identified in a screen for mutants with cell wall defects (8), and these results suggest a possible connection between Ecm5 function and cell wall maintenance. In response to stress, Snt2 and Ecm5 were also enriched at cellular transport genes (Fig. 4J) including the *FUI1* uridine permease (Fig. 5A), consistent with the enrichment of a motif similar to that of the Pdr1 and Pdr3 transport gene regulators among Snt2/Ecm5 target sites. Notably,

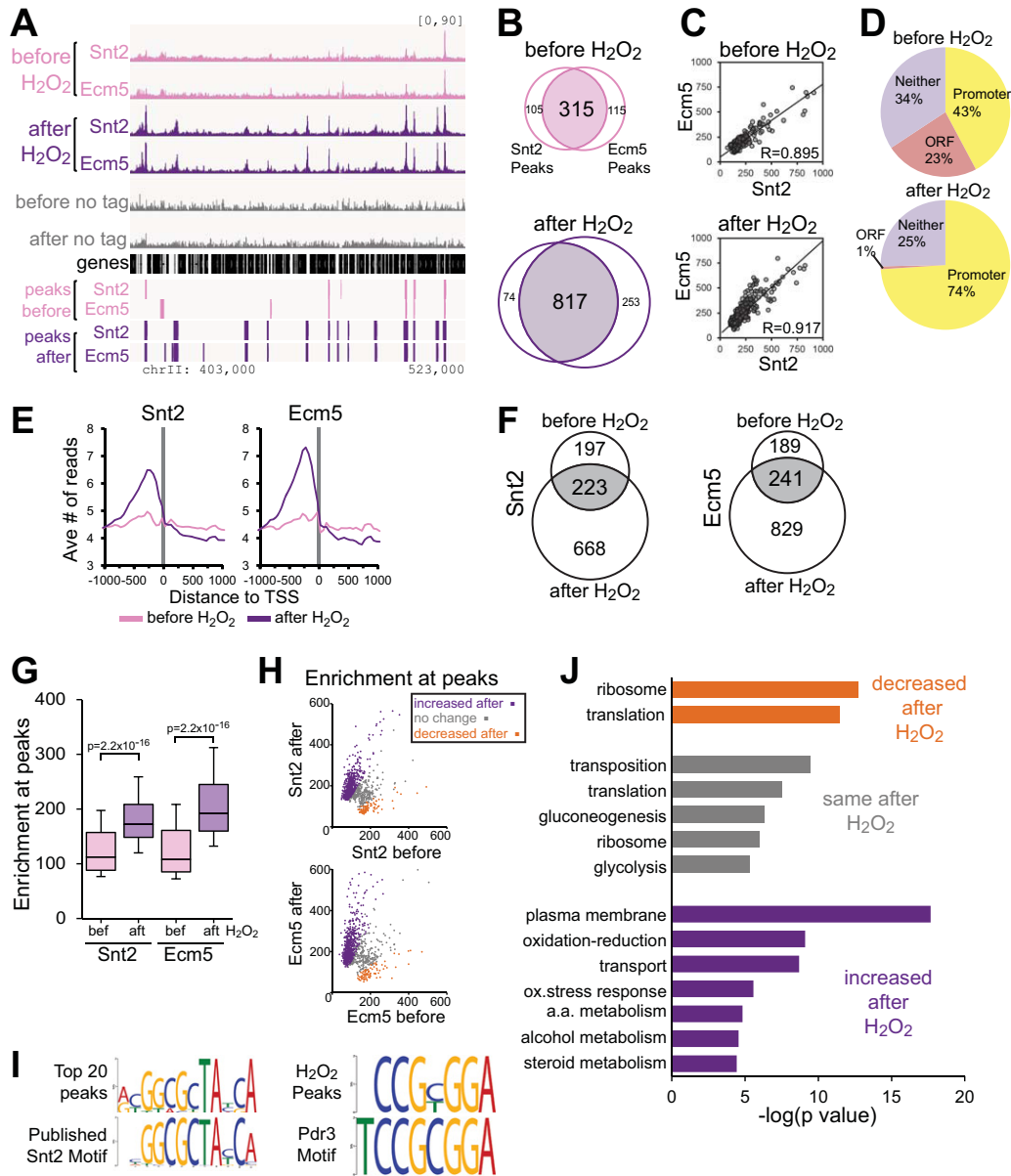


FIG 4 Snt2 and Ecm5 are highly colocalized and associate with additional promoters after H₂O₂ stress. (A) ChIP-seq tracks showing Snt2 and Ecm5 ChIP enrichment in a representative region before and after H₂O₂ treatment. The coverage values for each track are scaled by 1,000,000/number of reads, and the scale of the y axes for all tracks is shown in brackets. The locations of genes and peaks and the chromosomal coordinates are shown under the tracks. chrII, chromosome II. (B) Venn diagrams show that the majority of Snt2 and Ecm5 ChIP peaks overlap. (C) Correlations between Snt2 and Ecm5 enrichment before and after H₂O₂ treatment (Pearson's correlation coefficients are indicated in the bottom right-hand corners of the graphs). (D) Genomic distributions of shared Snt2/Ecm5 peaks before and after H₂O₂ stress. (E) Average number of Snt2 or Ecm5 ChIP-seq reads per 50-bp window around transcription start sites (TSSs) for all yeast genes, scaled by 1,000,000/total reads. (F) Overlaps of Snt2 or Ecm5 peaks before and after H₂O₂ treatment. (G) Box-and-whisker plots showing the distributions of Snt2 and Ecm5 enrichment at all peak regions before and after H₂O₂ treatment in the treated and untreated data sets. The bottoms, middles, and tops of the boxes depict the 25th, 50th, and 75th percentiles, respectively, and the top and bottom whiskers depict the 10th and 90th percentiles, respectively, of Snt2 or Ecm5 enrichment levels. The *P* values were determined by Wilcoxon rank sum test. (H) Snt2 or Ecm5 enrichment levels at peaks after H₂O₂ treatment relative to the levels before treatment. Peaks where Snt2/Ecm5 enrichment was >1.5-fold increased, >1.5-fold decreased, or unchanged after treatment are colored purple, orange, or gray, respectively. (I) Motif analysis using the 20 most-enriched Snt2/Ecm5 peaks (left) or all peaks where Snt2/Ecm5 levels increased after treatment (right). (J) Categories of genes significantly enriched by GO analysis of Snt2/Ecm5 peaks that increased, decreased, or did not change enrichment after treatment. ox.stress response, oxidative stress response; a.a. metabolism, amino acid metabolism.

ergosterol biosynthesis, amino acid metabolism, and cellular transport genes are all categories regulated as part of the environmental stress response (ESR) (1), showing that in response to stress, Snt2 and Ecm5 target ESR genes.

Consistent with genetic evidence linking Snt2 to oxidative

stress regulation, genes involved in redox reactions and the oxidative stress response also had increased levels of Snt2 and Ecm5 after treatment (Fig. 4J). These genes included *CYC1*, which encodes the cytochrome *c* component of the mitochondrial electron transport chain, and *SUE1*, which encodes a protein that degrades

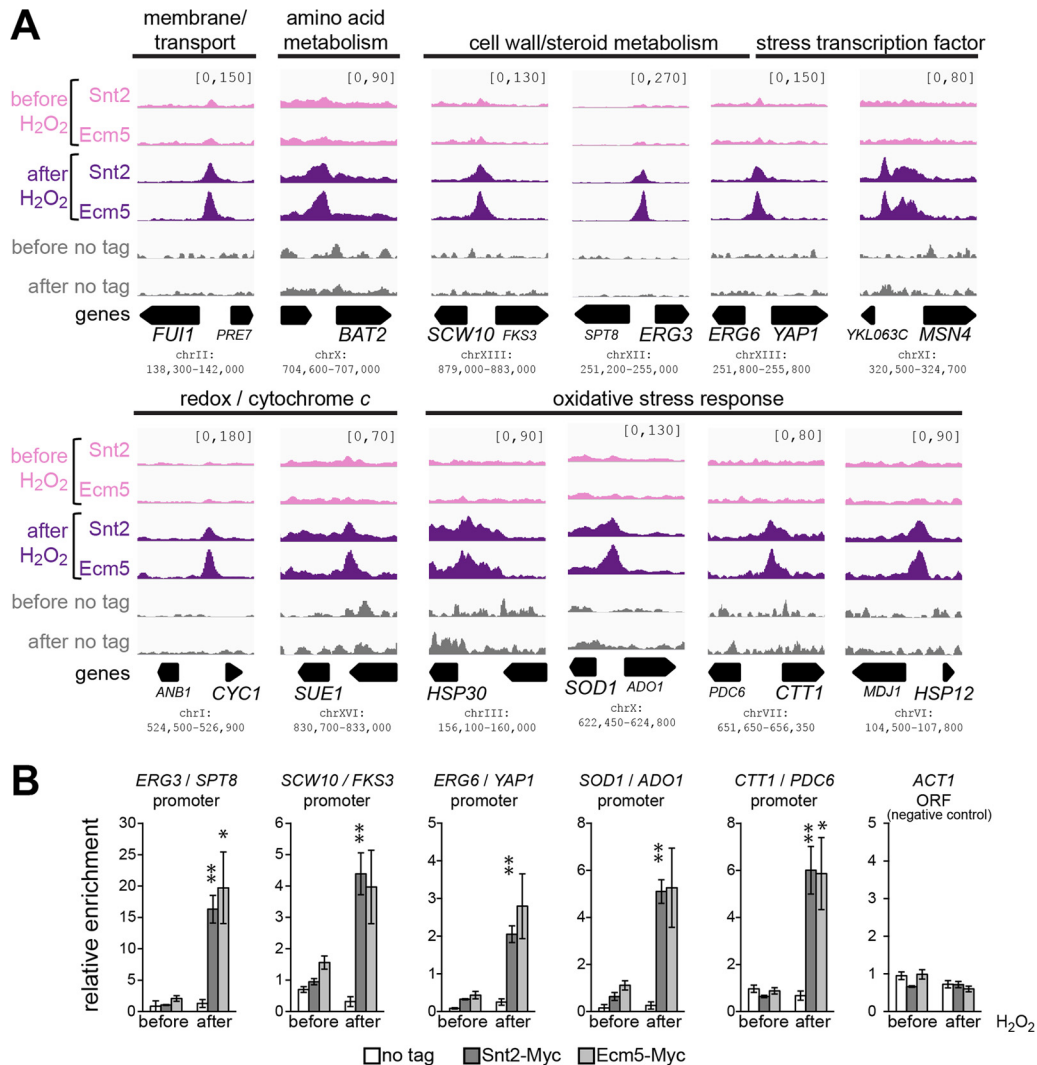


FIG 5 After H₂O₂ treatment, Snt2 and Ecm5 localize to stress and metabolism genes. (A) Examples of ESR genes whose promoters are enriched for Snt2 and Ecm5 after H₂O₂ treatment. For bidirectional promoters, the gene associated with the category above the panel is shown in a larger font. (B) ChIP-seq results were confirmed by ChIP-qPCR. Relative enrichment was determined by normalizing percent inputs at the target locus to percent inputs at a control region on the right arm of telomere 6. The means ± SEMs of 3 biological replicates are shown. Samples in which the ChIP enrichment after treatment differs significantly from enrichment before treatment are indicated by asterisks as follows: *, $P < 0.05$; **, $P < 0.01$. Enrichment in the *ACT1* ORF is shown as a negative control.

unstable cytochrome *c* (Fig. 5A). The incomplete reduction of oxygen in the electron transport chain is one of the main endogenous sources of ROS in cells (51), and the association of Snt2 and Ecm5 with promoters of genes involved in cytochrome *c* biology further links these proteins to oxidative stress. In addition, after H₂O₂ treatment, Snt2 and Ecm5 were enriched in the promoters of the genes encoding the oxidative stress transcription factors Yap1 and Cin5 (also known as Yap4) which are activated by oxidative stress (52, 53), the catalase Ctt1, and the superoxide dismutase Sod1, which detoxify ROS (54), as well as the membrane proteins Hsp30 and Hsp12, which are induced in response to oxidative stress (55, 56) (Fig. 5A and data not shown). Increased Snt2 and Ecm5 localization to many of these promoters in response to H₂O₂ treatment was confirmed by ChIP-qPCR (Fig. 5B and data not shown).

A small number of promoters were very highly enriched for Snt2 and Ecm5. ChIP-seq analysis identified a small set of pro-

motors very highly enriched for Snt2 and Ecm5 both before and after H₂O₂ treatment: while most peaks of Snt2 and Ecm5 enrichment had peak heights between 70 and 150 (representing the number of reads in the peak summit scaled by 1,000,000/total number of reads in that ChIP-seq experiment), we identified 10 “superenriched” Snt2 and Ecm5 peaks in the promoters of 14 genes, with peak heights over 500 in both untreated and treated cells (Table 3). For example, Snt2/Ecm5 peaks at the promoters of *CYC3/CDC19*, *BNR1/POT1*, and *MSN1* were more than 10-fold more enriched than the peaks described in the previous section (compare the values within brackets in Fig. 6A with those in Fig. 5A). Independent ChIP-qPCR experiments recapitulated the high levels of Snt2 and Ecm5 enrichment found at these promoters (Fig. 6B), showing that these high enrichment levels are not merely sequencing artifacts.

While the only significant GO association found for the 14 superenriched target genes was polysaccharide catabolism ($P =$

TABLE 3 Genes whose promoters were superenriched for Snt2 and Ecm5

Peak	Gene	Function
1	<i>CYC3</i>	Cytochrome c heme lyase
	<i>CDC19</i>	Pyruvate kinase
2	<i>SSA3</i>	HSP70 family chaperone involved in the stress response
3	<i>POT1</i>	Thiolase involved in beta-oxidation of fatty acids
	<i>BNR1</i>	Formin involved in actin polymerization
4	<i>PGU1</i>	Secreted polygalacturonase used to hydrolyze plant pectins
5	<i>STM1</i>	Ribosome-binding protein required for translation under nutrient stress
	<i>YLR149C</i>	Unknown
6	<i>IPI3</i>	Component of Rix1 complex involved in rRNA processing
	<i>YNL181W</i>	Putative oxidoreductase
7	<i>MSN1</i>	Transcriptional activator involved in the stress response
8	<i>CUP9</i>	Transcriptional repressor of <i>PTR2</i> peptide transporter gene
9	<i>CUR1</i>	Protein sorting factor induced in stressed cells
10	<i>GDB1</i>	Glycogen debranching enzyme involved in glycogen degradation

2.7×10^{-5}), likely due to the small number of genes, almost all of the genes had functions connected to the ESR (Table 3), including genes involved in carbohydrate metabolism (*GDB1*, *CDC19*, and *PGU1*), fatty acid metabolism (*POT1*), ribosome biogenesis (*IPI3*), translation (*STM1*), amino acid transport (*CUP9*), redox

reactions (*YNL181W* and *CYC3*), and general stress response (*SSA3*, *CUR1*, and *MSN1*). The high levels of Snt2 and Ecm5 at superenriched promoters may reflect high occupancy of these regions in all cells, or alternatively, a high proportion of cells in the culture that have Snt2 and Ecm5 occupied at these sites.

Snt2 and Ecm5 are required for Rpd3 recruitment to superenriched promoters but not for recruitment of the Rpd3(L) complex member Sds3. Because Rpd3 physically associated with Snt2 and Ecm5, we next determined whether Rpd3 also associated at Snt2/Ecm5 targets, and if so, whether it did so in an Snt2- or Ecm5-dependent manner. Deletion of *ECM5* or *SNT2* from a Myc-tagged Rpd3 strain did not alter global levels of Rpd3-Myc before or after H_2O_2 treatment (Fig. 6C). By ChIP-qPCR, Myc-tagged Rpd3 was enriched at all Snt2/Ecm5 target promoters assayed, both before (data not shown) and after (Fig. 6D) treatment. Surprisingly, deletion of *SNT2* or *ECM5* abrogated Rpd3-Myc enrichment at Snt2/Ecm5 superenriched promoters but not at promoters where Snt2 and Ecm5 were enriched after H_2O_2 treatment (Fig. 6D). Thus, there are at least two classes of Snt2/Ecm5 targets, those at which Snt2 and Ecm5 localize at high levels regardless of stress and recruit Rpd3, and those at which Snt2 and Ecm5 associate in response to H_2O_2 treatment, independently of Rpd3.

Because Rpd3 recruitment can also occur through association with the Rpd3(L) complex and Rpd3(L) function has been linked to the yeast stress response (11–16), we sought additional confirmation that the Snt2- and Ecm5-dependent association of Rpd3 with superenriched promoters occurred independently of the

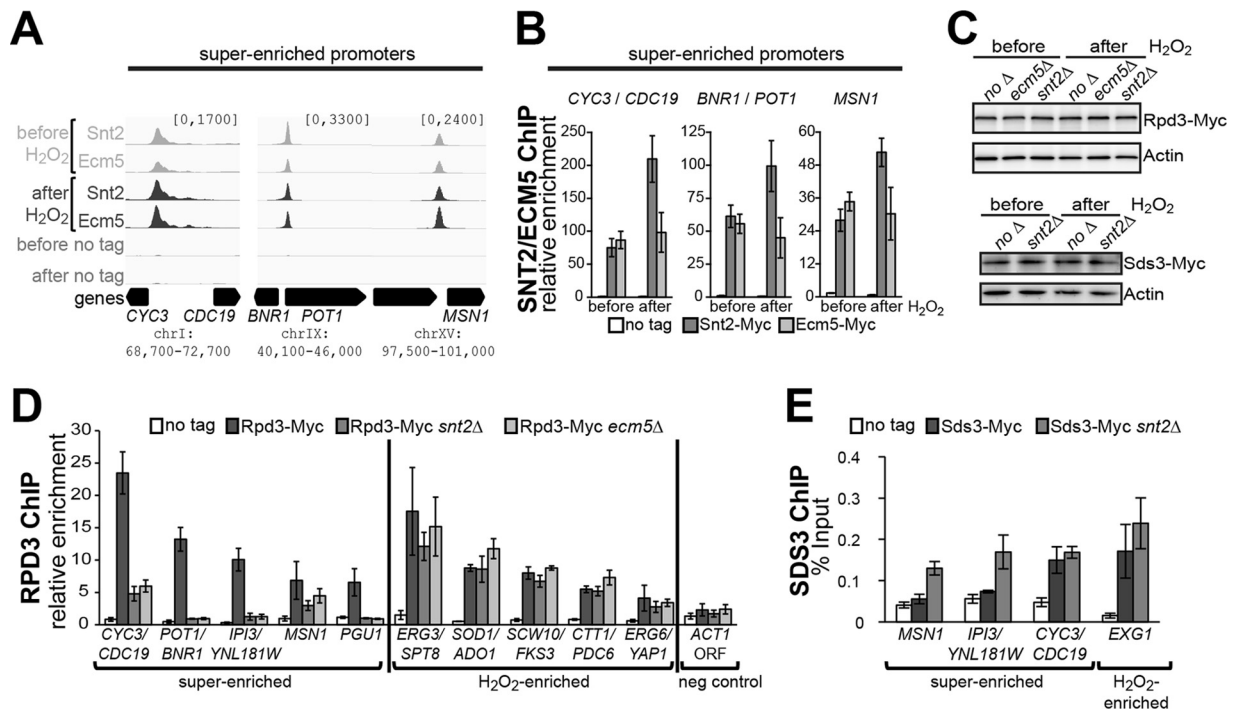


FIG 6 Snt2 and Ecm5 are required for Rpd3 recruitment to superenriched promoters but not for recruitment of the Rpd3(L) complex member Sds3. (A) Promoters superenriched for Snt2 and Ecm5 (note the ranges in brackets for ChIP-seq tracks) before and after H_2O_2 treatment. (B) ChIP-qPCR confirmation of high levels of Snt2 and Ecm5 at superenriched promoters shown in panel A. Data were normalized as described in the legend to Fig. 5B. (C) Control immunoblots showing that deletion of *SNT2* or *ECM5* did not affect Rpd3-Myc levels and that deletion of *SNT2* did not affect Sds3-Myc levels before or after H_2O_2 treatment. Actin blots serve as a loading controls. (D) Rpd3-Myc ChIP-qPCR performed on untagged, *RPD3-MYC*, *RPD3-MYC snt2Δ*, or *RPD3-MYC ecm5Δ* strains that were treated with H_2O_2 . Data were normalized as described in the legend to Fig. 5B. *ACT1* ORF is the negative control. (E) Sds3-Myc ChIP-qPCR performed on untagged, *SDS3-MYC*, or *SDS3-MYC snt2Δ* strains that were treated with H_2O_2 . Values are means \pm standard deviations of 3 independent measurements and are representative of 2 experiments.

Rpd3(L) complex. We tagged the Rpd3(L) subunit Sds3 with the Myc tag (Sds3-Myc) and used ChIP-qPCR to analyze Sds3-Myc association with Snt2/Ecm5 target promoters in the presence or absence of Snt2. Deletion of *SNT2* did not affect Sds3-Myc protein levels before or after H₂O₂ treatment (Fig. 6C). Sds3-Myc was not enriched above background levels at the *MSN1* or *IPI3/YNL181W* Snt2/Ecm5 superenriched promoters (Fig. 6E), suggesting that at these targets, Snt2, Ecm5, and Rpd3 function independently from the Rpd3(L) complex. Sds3-Myc was modestly enriched at the superenriched *CYC3/CDC19* promoter. However, Sds3-Myc enrichment of these promoters and the *EXG1* promoter, an H₂O₂-enriched Snt2/Ecm5 target, was not decreased when *SNT2* was deleted, showing that Snt2 and Ecm5 do not recruit Rpd3(L) to target promoters (Fig. 6E).

Snt2, but not Ecm5, is required for proper expression of ChIP target genes. Having shown that Snt2 and Ecm5 localize to ESR genes after H₂O₂ treatment, we next sought to determine whether Snt2 or Ecm5 regulated target gene expression. We performed RNA-sequencing (RNA-seq) analysis of wild-type, *snt2Δ*, or *ecm5Δ* strains before or 30 min after H₂O₂ treatment. The RNA-seq analysis was performed on three replicate samples, and expression levels of many Snt2 and Ecm5 target genes were confirmed by qPCR analysis (data not shown). In wild-type cells, 3,127 genes significantly changed expression in response to H₂O₂ treatment (significance determined by the CuffDiff program). A previous microarray study reported 1,294 genes up- or downregulated at least 2-fold in wild-type cells 30 min after treatment with 0.32 mM H₂O₂ (1). The larger number of genes identified in our study may reflect the higher sensitivity of the RNA-seq technique to identify transcription changes (CuffDiff can call fold differences below 2-fold significant if there are enough reads for the model to statistically call a difference) or possibly differences in the concentrations of H₂O₂ used in the two studies (0.4 mM in ours, compared to 0.32 mM in the previous study). Importantly, 1,030 of the 1,294 genes (80%) identified in the previous study were also up- or downregulated in response to H₂O₂ treatment in our study ($P < 3 \times 10^{-15}$ by hypergeometric test), confirming that the H₂O₂ treatment triggered changes in expression similar to the previously reported changes.

As expected, both before and after treatment, *ECM5* and *SNT2* were the genes most downregulated in the *ecm5Δ* and *snt2Δ* strains, respectively. Deletion of *ECM5* had minimal effects on gene expression: before treatment, only 33 genes differed in expression from wild-type levels, and only 7 genes differed from wild-type levels after treatment (Fig. 7A). In contrast, in the *snt2Δ* strain, 38 genes were downregulated and 134 genes upregulated relative to wild-type levels before H₂O₂ treatment, and 262 and 475 genes were down- and upregulated, respectively, relative to wild-type levels after treatment (Fig. 7A). Few genes showed expression changes in both the *snt2Δ* and *ecm5Δ* strains. Notably, two cell wall mannoprotein genes, *FIT1* and *DAN1*, showed opposite expression changes in the two strains (Fig. 7B). These results again link Snt2 and Ecm5 function to cell wall regulation and are consistent with Snt2 and Ecm5 having opposing functions.

Like the genes targeted by Snt2 and Ecm5 in response to H₂O₂, the genes up- or downregulated in the *snt2Δ* strain functioned in stress and metabolism pathways. Before H₂O₂ treatment, GO analysis identified genes involved in acetyl coenzyme A (acetyl-CoA) metabolism, NAD metabolism, oxidation-reduction processes, and the tricarboxylic acid cycle enriched among genes

whose expression changed in the *snt2Δ* strain (P values of 8.8×10^{-7} , 5.5×10^{-5} , 1.3×10^{-6} , and 5.8×10^{-8} , respectively). After H₂O₂ treatment, genes upregulated in the *snt2Δ* strain functioned in protein synthesis, rRNA processing, and hexose transport, while genes downregulated in the *snt2Δ* strain functioned in translation, amino acid metabolism, ROS metabolism, and response to ROS (Fig. 7C), further linking Snt2 to oxidative stress and metabolism regulation.

By integrating our RNA-seq and ChIP-seq analyses, we identified 403 of the 1,205 H₂O₂-enriched Snt2/Ecm5 target genes that were up- or downregulated at least 1.5-fold in the *snt2Δ* strain after treatment. Of the 403 genes, 309 genes also exhibited changes in expression in wild-type cells in response to H₂O₂ treatment (Fig. 7D), demonstrating considerable overlap between target genes directly regulated by Snt2 and target genes regulated through the oxidative stress response. Notably, many of the Snt2 and Ecm5 targets involved in the oxidative stress response or in cytochrome *c* regulation described above had altered expression levels in the *snt2Δ* strain after treatment (Fig. 7E). Taken together, these results show that H₂O₂ treatment prompts Snt2 to target and regulate stress response genes.

When the 309 target genes regulated by Snt2 were clustered on their expression profiles, 4 clusters could be distinguished, encompassing genes whose expression increased (clusters 1 and 2) or decreased (clusters 3 and 4) in wild-type cells after H₂O₂ treatment and genes whose expression levels in the *snt2Δ* strain after treatment were higher (clusters 1 and 3) or lower (clusters 2 and 4) than wild-type expression levels (Fig. 7F). While a regulatory trend was not readily observed when all 309 genes were considered together (Fig. 7G), distinct patterns did emerge within specific categories of genes. For instance, all but one of the 24 translation genes in this set were downregulated in the *snt2Δ* strain after treatment. In contrast, 38 of the 48 plasma membrane genes in this set were upregulated in the absence of Snt2, as were all 20 of the lipid metabolism genes, including the ergosterol metabolism genes.

Our expression results suggest that Snt2 functions to both promote and repress gene expression, depending on the target. A mechanism through which this might occur may be through Snt2-mediated stabilization of unique sets of transcriptional regulators at different genes. As mentioned above, a subset of H₂O₂-enriched Snt2/Ecm5 target promoters contained a motif similar to the motif of the Pdr1 and Pdr3 transcriptional regulators. To search for other transcription factors that might cooperate with Snt2, we used the YEASTRACT program (42) to search for factors with binding sites in the 309 Snt2-regulated target genes that exhibited changes in expression in wild-type cells in response to stress (Fig. 7H) and found that 205 of the 309 genes are targets of the Ste12 transcription factor, which is activated downstream of the Fus3 mating and Kss1 filamentous grown MAPK pathways and is also activated by nutrient stress (57). In addition, 138 of the 309 genes were targets of Rap1, which functions as both a transcriptional activator and repressor depending on the target (58), and regulates ribosomal biogenesis genes (59). Thus, Ste12 and Rap1 may be two additional factors that potentially cooperate with Snt2 to regulate gene expression.

Treatment with the TOR pathway inhibitor rapamycin promotes Snt2 and Ecm5 localization to many of the same genes as H₂O₂ treatment. The genes regulated by Snt2 and targeted by Snt2 and Ecm5 after H₂O₂ treatment had numerous functions linked to stress response, including genes involved in metabolism and nu-

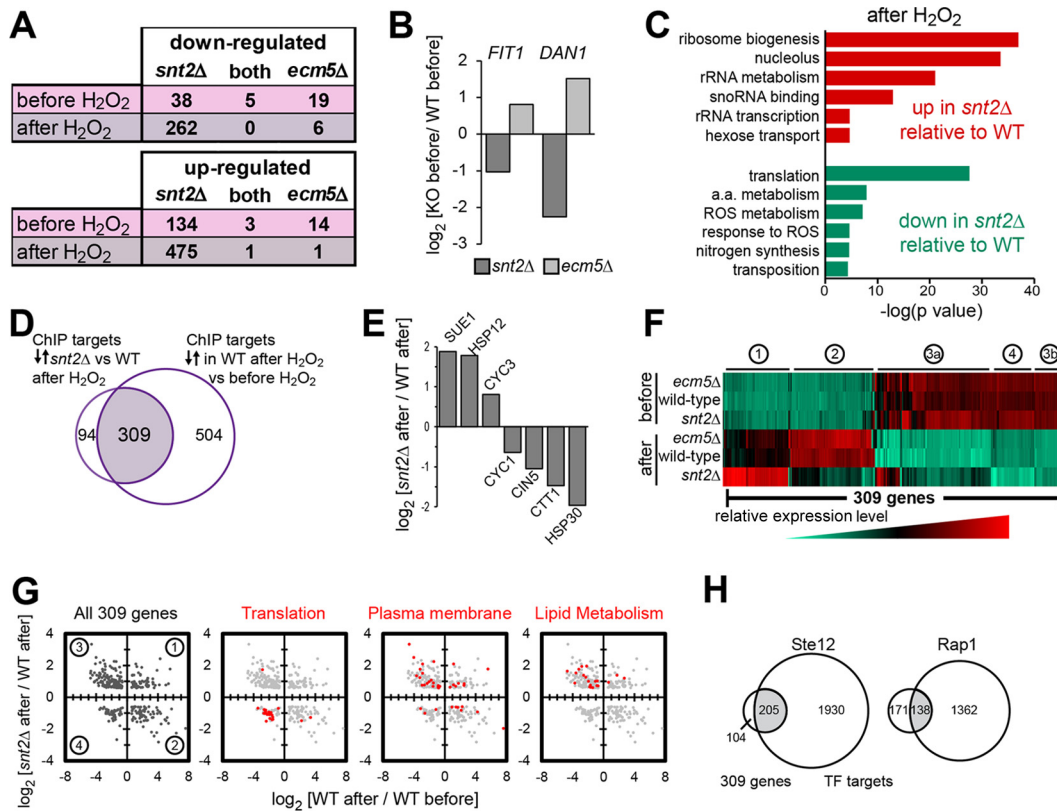


FIG 7 Snt2 is required for proper expression of ChIP target genes after H₂O₂ treatment. (A) Numbers of genes significantly up- or downregulated from wild-type (WT) levels in the *snt2Δ* or *ecm5Δ* strains before and after H₂O₂ treatment. (B) Two cell wall genes misexpressed in opposite ways in the *snt2Δ* and *ecm5Δ* strains. The graph shows log₂ ratios of expression in the mutant (knockout [KO]) strains relative to the WT levels before treatment. (C) Categories of genes significantly up- or downregulated in the *snt2Δ* strain relative to wild-type levels after H₂O₂ treatment. (D) Overlap between Snt2/Ecm5 H₂O₂-enriched target genes that were up- or downregulated relative to WT levels in the *snt2Δ* strain after treatment and target genes that changed expression in the WT strain after treatment. (E) Target genes that function in either the oxidative stress response or the cytochrome *c* pathway that were up- or downregulated in the *snt2Δ* strain after treatment. The graph shows log₂ ratios of expression levels in the *snt2Δ* strain after treatment relative to WT levels after treatment. (F) Heat map showing expression levels of the 309 genes described above for panel D. Four clusters of genes with similar expression patterns are noted at the top of the heat map. (G) Scatterplots of the 309 genes described above for panel D, comparing the log₂ expression ratios in *snt2Δ* cells after treatment relative to WT levels after treatment (y axis) to the log₂ expression ratios in WT cells after treatment relative to WT levels before treatment (x axis). In the three right scatterplots, genes in the categories above the plots are colored red. (H) Overlap between the 309 genes described above for panel D and Ste12 or Rap1 target genes. TF targets, transcription factor targets.

trient transport. We therefore hypothesized that rather than functioning solely in the oxidative stress response, Snt2 might function more broadly to regulate stress and metabolism. To test this, we interrogated the growth of the *snt2Δ* strain in the presence of rapamycin, a TOR pathway inhibitor that mimics nitrogen starvation (60). In dilution spotting assays, *snt2Δ* cells were resistant to rapamycin (Fig. 8A) (the less nutrient-rich SD CSM medium was chosen for these assays to ensure that the high levels of nutrients in YPD medium did not compensate for a nutrient stress phenotype).

We used ChIP-seq to map Snt2 and Ecm5 localization in cells treated for 30 min with rapamycin or with DMSO as a control. Similar to H₂O₂ treatment, rapamycin treatment prompted increased Snt2 and Ecm5 association at multiple loci (marked with small black arrows in Fig. 8B). Of the 155 Snt2/Ecm5 peaks where Snt2 and Ecm5 levels increased at least 1.5-fold in response to rapamycin treatment, 116 were also regions where Snt2/Ecm5 levels increased after H₂O₂ treatment (Fig. 8C). For example, both H₂O₂ and rapamycin treatment prompted Snt2 and Ecm5 enrichment at the promoters of the *FUI1* uridine permease and *BAT2* amino acid aminotransferase genes (Fig. 8D). These results sug-

gest that rather than Snt2 being a unique regulator of oxidative stress, Snt2 regulates stress and metabolism more broadly.

DISCUSSION

All cells must balance allocation of energy to growth with allocation to stress defense mechanisms, and when cells are exposed to stress, they must rapidly shift investment to the latter. In yeast, this shift involves regulation of a common set of genes called the ESR genes (1, 2). However, the mechanisms through which these genes are regulated are not fully understood. Here, we have shown that Snt2 physically associates with Ecm5 and the Rpd3 deacetylase and have integrated phenotypic, ChIP-seq, and RNA-seq analyses to uncover an Rpd3-independent role for Snt2 in regulating genes in response to oxidative stress. While a previous study mapped Snt2 localization using ChIP-chip (6), as far we know, ours is the first study to map Snt2 using high-throughput sequencing, and more importantly, the first to examine the localization changes of either Snt2 or Ecm5 in response to stress.

Consistent with a previous report (7), our LC-MS analysis of affinity-purified PrA-tagged Snt2, Ecm5, and Rpd3 cell lysates confirmed associations between these three proteins (Fig. 1 and

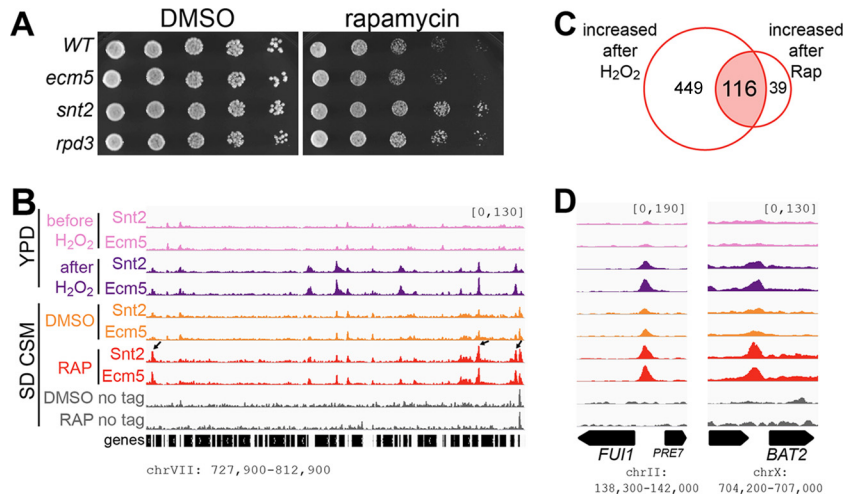


FIG 8 Rapamycin treatment recapitulates a subset of the Snt2 and Ecm5 localization changes seen after H_2O_2 treatment. (A) Serial dilutions of the indicated WT or knockout strains were spotted onto SD CSM plates supplemented with DMSO alone or rapamycin dissolved in DMSO (50 nM final concentration). (B) Snt2/Ecm5 ChIP-seq enrichment in control and rapamycin (RAP)-treated cells at a representative region on chromosome VII. Arrows indicate regions where Snt2 and Ecm5 levels were enriched after rapamycin treatment. (C) Overlap between peaks where the levels of Snt2 and Ecm5 were at least 1.5-fold higher after rapamycin treatment and peaks where Snt2/Ecm5 levels were higher after H_2O_2 treatment. (D) Promoters enriched for Snt2 and Ecm5 after H_2O_2 or rapamycin treatment.

Table 2; see Data set S1 in the supplemental material). While Rpd3 is known to associate with two other complexes (9, 10), we did not identify subunits of either complex associating with Snt2 or Ecm5 (Fig. 1D and Table 2; see Data set S1), suggesting that Snt2, Ecm5, and Rpd3 comprise a third Rpd3 complex.

Strikingly, both the *snt2Δ* and *rpd3Δ* strains were resistant to H_2O_2 -mediated oxidative stress (Fig. 2A and B), leading us to initially hypothesize that Snt2, Ecm5, and Rpd3 functioned together in the oxidative stress response. We used ChIP-seq to identify regions where Snt2 and Ecm5 were localized before and 30 min after H_2O_2 treatment (Fig. 4) and surprisingly, identified at least two distinct types of Snt2/Ecm5 targets: a small number of promoter regions at which Snt2 and Ecm5 are required for Rpd3 localization (Fig. 6) and a much larger set of promoters where Snt2 and Ecm5 localize independently of Rpd3 in response to H_2O_2 treatment (Fig. 5).

In the first set of promoters, high levels of Snt2 and Ecm5 were detected in both untreated and H_2O_2 -treated cells (Fig. 6A and B and Table 3). Rpd3 was enriched at these promoters, and Snt2 and Ecm5 were required for Rpd3 enrichment (Fig. 6D and data not shown). Consistent with our inability to detect Rpd3(L) subunits associating with Snt2 and Ecm5, deletion of *SNT2* did not affect the localization of the Rpd3(L) complex member Sds3 (Fig. 6E), further supporting the idea that Snt2, Ecm5, and Rpd3 function as a distinct complex. While many of the superenriched promoters had functions linked to stress response, Snt2, Ecm5, and Rpd3 associated with these regions before and after H_2O_2 treatment. Furthermore, we did not detect altered levels of Snt2-GFP, Ecm5-Myc, and Rpd3 associating with one another after H_2O_2 treatment (Fig. 3), suggesting that Snt2, Ecm5, and Rpd3 may have a stress-independent function at these promoters. Surprisingly, while deletion of *SNT2* or *ECM5* decreased Rpd3 levels at these promoters, we did not detect changes in histone H3 acetyl levels in these regions by ChIP-qPCR (data not shown). Rpd3 may be recruited to these regions to deacetylate other histone substrates or nonhistone proteins. Alternatively, association of Rpd3 with Snt2 and

Ecm5 may inactivate it. Consistent with the latter hypothesis, in *Drosophila*, association of Rpd3 with a complex containing the Ecm5 homolog Lid was reported to inhibit deacetylase activity (61).

We identified a second set of promoters where levels of Snt2 and Ecm5 increased after H_2O_2 stress (Fig. 4H and 5). While Rpd3 was enriched at these promoters by ChIP-qPCR, deletion of *SNT2* or *ECM5* did not affect Rpd3 association (Fig. 6D), suggesting that other proteins recruit Rpd3 to these targets. The Rpd3(L) complex regulates genes in response to diverse stresses (13–16), including oxidative stress (12), and may recruit Rpd3 to these regions. RNA-seq analysis identified 309 H_2O_2 -enriched target genes that changed expression in wild-type cells in response to H_2O_2 and were either up- or downregulated when *SNT2* was deleted (Fig. 7D), many of which function in oxidative stress response or oxidative metabolism (Fig. 7E).

While initially surprising that Snt2 might function as both an activator and a repressor, a number of other yeast transcriptional regulators, including Hap1 and Rap1, have been reported to have dual roles in transcription (58, 62, 63). The methods through which these proteins exert such opposing effects remain to be elucidated, but they may involve the cooperation of unique factors at different promoters. A subset of the H_2O_2 -enriched promoters contained a motif similar to the known Pdr1/Pdr3 motif (Fig. 4I), and many of the Snt2/Ecm5 target genes regulated by Snt2 are also known to be targeted by Ste12 and Rap1 (Fig. 7H), suggesting that Pdr3, Pdr1, Ste12, and Rap1 may cooperate with Snt2 to regulate different gene sets.

Surprisingly, despite the physical association and genomic colocalization of Snt2 and Ecm5, our genetic data uncovered independent functions for these proteins in the response to H_2O_2 stress. Unlike the *snt2Δ* strain, the *ecm5Δ* strain was not resistant to oxidative stress (Fig. 2A and B) and had few gene expression changes (Fig. 7A), but deletion of the *ECM5* gene from the *snt2Δ* strain reversed the H_2O_2 resistance of this strain (Fig. 2C), suggesting that Ecm5 has a function that is opposed to that of Snt2. In

support of this, the synthetic sickness of the *ecm5Δ ask10Δ* double mutant (17) suggests that Ecm5 function promotes oxidative stress tolerance, while Snt2 function ultimately decreases tolerance.

Because Snt2 and Ecm5 localized to genes that function in multiple pathways linked to the ESR, and not just to oxidative stress response genes, we hypothesized that rather than regulating only the oxidative stress pathway, Snt2 regulates stress pathways more broadly. In support of this, the *snt2Δ* strain was resistant to rapamycin (Fig. 8A), and rapamycin treatment promoted Snt2 and Ecm5 association with a subset of the H₂O₂ target promoters (Fig. 8C and D). A recent study reported that an *snt2Δ* strain was sensitive to histone overexpression (64). While the authors of that study propose that Snt2 functions in histone degradation, their results could also be explained if altered stress regulation in *snt2Δ* cells renders the cells more sensitive to the stress of histone overexpression.

The mechanism through which Snt2 and Ecm5 localization is regulated remains an exciting question and could involve stress-specific protein associations, posttranslational modifications, or regulation of subcellular distribution. Along these lines, our LC-MS analysis identified a phosphorylation site on serine 641 of Snt2 (Table 2). However, mutation of this serine to alanine or glutamate did not prevent ectopic Snt2 from rescuing the *snt2Δ* phenotype (data not shown), suggesting that this residue is not required for stress-mediated Snt2 regulation. It is noteworthy that a recent protein localization study reported that Ecm5 localized to the nucleus, while Snt2 localized to both the cytoplasm and nucleus and accumulated in the nucleus after nitrogen starvation (65). While this study did not find a change in Snt2 localization after H₂O₂ stress, we note that a higher concentration of H₂O₂ was used than in our study, possibly activating different stress pathways. Future studies aimed at providing insights into the mechanisms of Snt2 and Ecm5 regulation will be of considerable interest.

ACKNOWLEDGMENTS

This work was supported by NIH grants CA09673 to L.A.B., GM40922 to C.D.A., and GM103314 and GM103511 to B.T.C. and B.M.U. and by The Rockefeller University.

We thank members of the Allis research laboratory for helpful discussions and especially thank Jung-Ae Kim, Kyung-Min Noh, Christina Hughes, and Laura Banaszynski for critical reading of the manuscript. We also thank Christopher Streeter and Charles Li for helpful discussions and computational assistance.

REFERENCES

- Gasch AP, Spellman PT, Kao CM, Carmel-Harel O, Eisen MB, Storz G, Botstein D, Brown PO. 2000. Genomic expression programs in the response of yeast cells to environmental changes. *Mol. Biol. Cell* 11:4241–4257.
- Causton HC, Ren B, Koh SS, Harbison CT, Kanin E, Jennings EG, Lee TI, True HL, Lander ES, Young RA. 2001. Remodeling of yeast genome expression in response to environmental changes. *Mol. Biol. Cell* 12:323–337.
- Morano KA, Grant CM, Moye-Rowley WS. 2012. The response to heat shock and oxidative stress in *Saccharomyces cerevisiae*. *Genetics* 190:1157–1195.
- de Nadal E, Ammerer G, Posas F. 2011. Controlling gene expression in response to stress. *Nat. Rev. Genet.* 12:833–845.
- Estruch F. 2000. Stress-controlled transcription factors, stress-induced genes and stress tolerance in budding yeast. *FEMS Microbiol. Rev.* 24:469–486.
- Harbison CT, Gordon DB, Lee TI, Rinaldi NJ, Macisaac KD, Danford TW, Hannett NM, Tagne JB, Reynolds DB, Yoo J, Jennings EG, Zeitlinger J, Pokholok DK, Kellis M, Rolfe PA, Takusagawa KT, Lander ES, Gifford DK, Fraenkel E, Young RA. 2004. Transcriptional regulatory code of a eukaryotic genome. *Nature* 431:99–104.
- Shevchenko A, Roguev A, Schafit D, Buchanan L, Habermann B, Sakalar C, Thomas H, Krogan NJ, Stewart AF. 2008. Chromatin Central: towards the comparative proteome by accurate mapping of the yeast proteomic environment. *Genome Biol.* 9:R167. doi:10.1186/gb-2008-9-11-r167.
- Lussier M, White AM, Sheraton J, di Paolo T, Treadwell J, Southard SB, Horenstein CI, Chen-Weiner J, Ram AF, Kapteyn JC, Roemer TW, Vo DH, Bondoc DC, Hall J, Zhong WW, Sdicu AM, Davies J, Klis FM, Robbins PW, Bussey H. 1997. Large scale identification of genes involved in cell surface biosynthesis and architecture in *Saccharomyces cerevisiae*. *Genetics* 147:435–450.
- Carrozza MJ, Li B, Florens L, Sugauma T, Swanson SK, Lee KK, Shia WJ, Anderson S, Yates J, Washburn MP, Workman JL. 2005. Histone H3 methylation by Set2 directs deacetylation of coding regions by Rpd3S to suppress spurious intragenic transcription. *Cell* 123:581–592.
- Keogh MC, Kurdistani SK, Morris SA, Ahn SH, Podolny V, Collins SR, Schuldiner M, Chin K, Punna T, Thompson NJ, Boone C, Emili A, Weissman JS, Hughes TR, Strahl BD, Grunstein M, Greenblatt JF, Buratowski S, Krogan NJ. 2005. Cotranscriptional set2 methylation of histone H3 lysine 36 recruits a repressive Rpd3 complex. *Cell* 123:593–605.
- Rundlett SE, Carmen AA, Kobayashi R, Bavykin S, Turner BM, Grunstein M. 1996. HDA1 and RPD3 are members of distinct yeast histone deacetylase complexes that regulate silencing and transcription. *Proc. Natl. Acad. Sci. U. S. A.* 93:14503–14508.
- Alejandro-Osorio AL, Huebert DJ, Porcaro DT, Sonntag ME, Nill-asithanukroh S, Will JL, Gasch AP. 2009. The histone deacetylase Rpd3p is required for transient changes in genomic expression in response to stress. *Genome Biol.* 10:R57. doi:10.1186/gb-2009-10-5-r57.
- De Nadal E, Zapater M, Alepuz PM, Sumoy L, Mas G, Posas F. 2004. The MAPK Hog1 recruits Rpd3 histone deacetylase to activate osmoreponsive genes. *Nature* 427:370–374.
- Kremer SB, Gross DS. 2009. SAGA and Rpd3 chromatin modification complexes dynamically regulate heat shock gene structure and expression. *J. Biol. Chem.* 284:32914–32931.
- Sertil O, Vemula A, Salmon SL, Morse RH, Lowry CV. 2007. Direct role for the Rpd3 complex in transcriptional induction of the anaerobic DAN/TIR genes in yeast. *Mol. Cell. Biol.* 27:2037–2047.
- Ruiz-Roig C, Vieitez C, Posas F, de Nadal E. 2010. The Rpd3L HDAC complex is essential for the heat stress response in yeast. *Mol. Microbiol.* 76:1049–1062.
- Collins SR, Miller KM, Maas NL, Roguev A, Fillingham J, Chu CS, Schuldiner M, Gebbia M, Recht J, Shales M, Ding H, Xu H, Han J, Ingvarsdottir K, Cheng B, Andrews B, Boone C, Berger SL, Hieter P, Zhang Z, Brown GW, Ingles CJ, Emili A, Allis CD, Toczyski DP, Weissman JS, Greenblatt JF, Krogan NJ. 2007. Functional dissection of protein complexes involved in yeast chromosome biology using a genetic interaction map. *Nature* 446:806–810.
- Cohen TJ, Lee K, Rutkowski LH, Strich R. 2003. Ask10p mediates the oxidative stress-induced destruction of the *Saccharomyces cerevisiae* C-type cyclin Ume3p/Srb11p. *Eukaryot. Cell* 2:962–970.
- Page N, Sheraton J, Brown JL, Stewart RC, Bussey H. 1996. Identification of ASK10 as a multicopy activator of Skn7p-dependent transcription of a HIS3 reporter gene. *Yeast* 12:267–272.
- de Groot PW, Ruiz C, Vazquez de Aldana CR, Duenas E, Cid VJ, Del Rey F, Rodriguez-Pena JM, Perez P, Andel A, Caubin J, Arroyo J, Garcia JC, Gil C, Molina M, Garcia LJ, Nombela C, Klis FM. 2001. A genomic approach for the identification and classification of genes involved in cell wall formation and its regulation in *Saccharomyces cerevisiae*. *Comp. Funct. Genomics* 2:124–142.
- Vilella F, Herrero E, Torres J, de la Torre-Ruiz MA. 2005. Pkc1 and the upstream elements of the cell integrity pathway in *Saccharomyces cerevisiae*, Rom2 and Mtl1, are required for cellular responses to oxidative stress. *J. Biol. Chem.* 280:9149–9159.
- Miller C, Schwalb B, Maier K, Schulz D, Dumcke S, Zacher B, Mayer A, Sydow J, Marcinowski L, Dolken L, Martin DE, Tresch A, Cramer P. 2011. Dynamic transcriptome analysis measures rates of mRNA synthesis and decay in yeast. *Mol. Syst. Biol.* 7:458. doi:10.1038/msb.2010.112.
- Longtine MS, McKenzie A, III, Demarini DJ, Shah NG, Wach A, Brachat A, Philippsen P, Pringle JR. 1998. Additional modules for ver-

- satite and economical PCR-based gene deletion and modification in *Saccharomyces cerevisiae*. *Yeast* 14:953–961.
24. Aitchison JD, Rout MP, Marelli M, Blobel G, Wozniak RW. 1995. Two novel related yeast nucleoporins Nup170p and Nup157p: complementation with the vertebrate homologue Nup155p and functional interactions with the yeast nuclear pore-membrane protein Pom152p. *J. Cell Biol.* 131:1133–1148.
 25. Ahn SH, Diaz RL, Grunstein M, Allis CD. 2006. Histone H2B deacetylation at lysine 11 is required for yeast apoptosis induced by phosphorylation of H2B at serine 10. *Mol. Cell* 24:211–220.
 26. Oeffinger M, Wei KE, Rogers R, DeGrasse JA, Chait BT, Aitchison JD, Rout MP. 2007. Comprehensive analysis of diverse ribonucleoprotein complexes. *Nat. Methods* 4:951–956.
 27. Cristea IM, Chait BT. 2011. Conjugation of magnetic beads for immunopurification of protein complexes. *Cold Spring Harb. Protoc.* 2011: pdb.prot5610. doi:10.1101/pdb.prot5610.
 28. Cristea IM, Chait BT. 2011. Affinity purification of protein complexes. *Cold Spring Harb. Protoc.* 2011: pdb.prot5611. doi:10.1101/pdb.prot5611.
 29. Craig R, Beavis RC. 2004. TANDEM: matching proteins with tandem mass spectra. *Bioinformatics* 20:1466–1467.
 30. Gavin AC, Bosche M, Krause R, Grandi P, Marzioch M, Bauer A, Schultz J, Rick JM, Michon AM, Cruciat CM, Remor M, Hofert C, Schelder M, Brajenovic M, Ruffner H, Merino A, Klein K, Hudak M, Dickson D, Rudi T, Gnau V, Bauch A, Bastuck S, Huhse B, Leutwein C, Heurtier MA, Copley RR, Edelmann A, Querfurth E, Rybin V, Drewes G, Raida M, Bouwmeester T, Bork P, Seraphin B, Kuster B, Neubauer G, Superti-Furga G. 2002. Functional organization of the yeast proteome by systematic analysis of protein complexes. *Nature* 415:141–147.
 31. Ghaemmaghami S, Huh WK, Bower K, Howson RW, Belle A, Dephoure N, O'Shea EK, Weissman JS. 2003. Global analysis of protein expression in yeast. *Nature* 425:737–741.
 32. Aparicio O, Geisberg JV, Sekinger E, Yang A, Moqtaderi Z, Struhl K. 2005. Chromatin immunoprecipitation for determining the association of proteins with specific genomic sequences in vivo. *Curr. Protoc. Mol. Biol.* Chapter 17:Unit 21.3. doi:10.1002/0471142727.mb2103s69.
 33. Collart MA, Oliviero S. 2001. Preparation of yeast RNA. *Curr. Protoc. Mol. Biol.* Chapter 13:Unit13.12. doi:10.1002/0471142727.mb1312s23.
 34. Langmead B, Trapnell C, Pop M, Salzberg SL. 2009. Ultrafast and memory-efficient alignment of short DNA sequences to the human genome. *Genome Biol.* 10:R25. doi:10.1186/gb-2009-10-3-r25.
 35. Zhang Y, Liu T, Meyer CA, Eeckhoutte J, Johnson DS, Bernstein BE, Nusbaum C, Myers RM, Brown M, Li W, Liu XS. 2008. Model-based analysis of ChIP-Seq (MACS). *Genome Biol.* 9:R137. doi:10.1186/gb-2008-9-9-r137.
 36. Goecks J, Nekrutenko A, Taylor J. 2010. Galaxy: a comprehensive approach for supporting accessible, reproducible, and transparent computational research in the life sciences. *Genome Biol.* 11:R86. doi:10.1186/gb-2010-11-8-r86.
 37. Blankenberg D, Von Kuster G, Coraor N, Ananda G, Lazarus R, Mangan M, Nekrutenko A, Taylor J. 2010. Galaxy: a web-based genome analysis tool for experimentalists. *Curr. Protoc. Mol. Biol.* Chapter 19: Unit 19.10.1-21. doi:10.1002/0471142727.mb1910s89.
 38. Giardine B, Riemer C, Hardison RC, Burhans R, Eltnitski L, Shah P, Zhang Y, Blankenberg D, Albert I, Taylor J, Miller W, Kent WJ, Nekrutenko A. 2005. Galaxy: a platform for interactive large-scale genome analysis. *Genome Res.* 15:1451–1455.
 39. Quinlan AR, Hall IM. 2010. BEDTools: a flexible suite of utilities for comparing genomic features. *Bioinformatics* 26:841–842.
 40. Berriz GF, Beaver JE, Cenik C, Tasan M, Roth FP. 2009. Next generation software for functional trend analysis. *Bioinformatics* 25:3043–3044.
 41. Bailey TL, Boden M, Buske FA, Frith M, Grant CE, Clementi L, Ren J, Li WW, Noble WS. 2009. MEME SUITE: tools for motif discovery and searching. *Nucleic Acids Res.* 37:W202–W208.
 42. Abdulrehman D, Monteiro PT, Teixeira MC, Mira NP, Lourenco AB, dos Santos SC, Cabrito TR, Francisco AP, Madeira SC, Aires RS, Oliveira AL, Sa-Correia I, Freitas AT. 2011. YEASTRACT: providing a programmatic access to curated transcriptional regulatory associations in *Saccharomyces cerevisiae* through a web services interface. *Nucleic Acids Res.* 39:D136–D140.
 43. Trapnell C, Pachter L, Salzberg SL. 2009. TopHat: discovering splice junctions with RNA-Seq. *Bioinformatics* 25:1105–1111.
 44. Trapnell C, Williams BA, Pertea G, Mortazavi A, Kwan G, van Baren MJ, Salzberg SL, Wold BJ, Pachter L. 2010. Transcript assembly and quantification by RNA-Seq reveals unannotated transcripts and isoform switching during cell differentiation. *Nat. Biotechnol.* 28:511–515.
 45. Robinson JT, Thorvaldsdottir H, Winckler W, Guttman M, Lander ES, Getz G, Mesirov JP. 2011. Integrative genomics viewer. *Nat. Biotechnol.* 29:24–26.
 46. Molin M, Yang J, Hanzen S, Toledano MB, Labarre J, Nystrom T. 2011. Life span extension and H(2)O(2) resistance elicited by caloric restriction require the peroxiredoxin Tsa1 in *Saccharomyces cerevisiae*. *Mol. Cell* 43:823–833.
 47. Schnell N, Krems B, Entian KD. 1992. The PAR1 (YAP1/SNQ3) gene of *Saccharomyces cerevisiae*, a c-jun homologue, is involved in oxygen metabolism. *Curr. Genet.* 21:269–273.
 48. Fan X, Struhl K. 2009. Where does mediator bind in vivo? *PLoS One* 4:e5029. doi:10.1371/journal.pone.0005029.
 49. Badis G, Chan ET, van Bakel H, Pena-Castillo L, Tillo D, Tsui K, Carlson CD, Gossett AJ, Hasinoff MJ, Warren CL, Gebbia M, Talukder S, Yang A, Mnaimneh S, Terterov D, Coburn D, Li Yeo A, Yeo ZX, Clarke ND, Lieb JD, Ansari AZ, Nislow C, Hughes TR. 2008. A library of yeast transcription factor motifs reveals a widespread function for Rsc3 in targeting nucleosome exclusion at promoters. *Mol. Cell* 32:878–887.
 50. Mamnun YM, Pandjaitan R, Mahe Y, Delahodde A, Kuchler K. 2002. The yeast zinc finger regulators Pdr1p and Pdr3p control pleiotropic drug resistance (PDR) as homo- and heterodimers in vivo. *Mol. Microbiol.* 46:1429–1440.
 51. Skulachev VP. 1998. Cytochrome c in the apoptotic and antioxidant cascades. *FEBS Lett.* 423:275–280.
 52. Kuge S, Jones N, Nomoto A. 1997. Regulation of yAP-1 nuclear localization in response to oxidative stress. *EMBO J.* 16:1710–1720.
 53. Nevitt T, Pereira J, Rodrigues-Pousada C. 2004. YAP4 gene expression is induced in response to several forms of stress in *Saccharomyces cerevisiae*. *Yeast* 21:1365–1374.
 54. Herrero E, Ros J, Belli G, Cabisco E. 2008. Redox control and oxidative stress in yeast cells. *Biochim. Biophys. Acta* 1780:1217–1235.
 55. Seymour IJ, Piper PW. 1999. Stress induction of HSP30, the plasma membrane heat shock protein gene of *Saccharomyces cerevisiae*, appears not to use known stress-regulated transcription factors. *Microbiology* 145: 231–239.
 56. Raitt DC, Johnson AL, Erkin AM, Makino K, Morgan B, Gross DS, Johnston LH. 2000. The Skn7 response regulator of *Saccharomyces cerevisiae* interacts with Hsf1 in vivo and is required for the induction of heat shock genes by oxidative stress. *Mol. Biol. Cell* 11:2335–2347.
 57. Rispaill N, Di Pietro A. 2010. The homeodomain transcription factor Ste12: connecting fungal MAPK signalling to plant pathogenicity. *Commun. Integr. Biol.* 3:327–332.
 58. Morse RH. 2000. RAP, RAP, open up! New wrinkles for RAP1 in yeast. *Trends Genet.* 16:51–53.
 59. Lieb JD, Liu X, Botstein D, Brown PO. 2001. Promoter-specific binding of Rap1 revealed by genome-wide maps of protein-DNA association. *Nat. Genet.* 28:327–334.
 60. Crespo JL, Hall MN. 2002. Elucidating TOR signaling and rapamycin action: lessons from *Saccharomyces cerevisiae*. *Microbiol. Mol. Biol. Rev.* 66:579–591.
 61. Lee N, Erdjument-Bromage H, Tempst P, Jones RS, Zhang Y. 2009. The H3K4 demethylase lid associates with and inhibits histone deacetylase Rpd3. *Mol. Cell. Biol.* 29:1401–1410.
 62. Hickman MJ, Winston F. 2007. Heme levels switch the function of Hap1 of *Saccharomyces cerevisiae* between transcriptional activator and transcriptional repressor. *Mol. Cell. Biol.* 27:7414–7424.
 63. Weiner A, Chen HV, Liu CL, Rahat A, Klien A, Soares L, Gudipati M, Pfeiffer J, Regev A, Buratowski S, Pleiss JA, Friedman N, Rando OJ. 2012. Systematic dissection of roles for chromatin regulators in a yeast stress response. *PLoS Biol.* 10:e1001369. doi:10.1371/journal.pbio.1001369.
 64. Singh RK, Gonzalez M, Kabbaj MH, Gunjan A. 2012. Novel E3 ubiquitin ligases that regulate histone protein levels in the budding yeast *Saccharomyces cerevisiae*. *PLoS One* 7:e36295. doi:10.1371/journal.pone.0036295.
 65. Breker M, Gymrek M, Schuldiner M. 2013. A novel single-cell screening platform reveals proteome plasticity during yeast stress responses. *J. Cell Biol.* 200:839–850.